ADVANCES IN INFOR

Quality of P

Security Measurem

SpringerWienNewYork

CISM COURSES AND LECTURES

The series presents lecture notes, monographs, edited works and proceedings in the field of Mechanics, Engineering, Computer Science and Applied Mathematics.
Purpose of the series is to make known in the international scientific and technical community results obtained in some of the activities organized by CISM, the International Centre for Mechanical Sciences.

INTERNATIONAL CENTRE FOR MECHANICAL SCIENCES

COURSES AND LECTURES – No. 487

ROMANSY 16

ROBOT DESIGN, DYNAMICS, AND CONTROL

EDITED BY

TERESA ZIELIŃSKA, CEZARY ZIELIŃSKI
WARSAW UNIVERSITY OF TECHNOLOGY

SpringerWienNewYork

This volume contains 292 illustrations and 34 tables

Printed in Poland
SPIN 11791393

In order to make this volume available as economically and as rapidly as possible the authors' type scripts have been reproduced in their original forms. This method unfortunately has its typographical limitations but it is hoped that they in no way distract the reader.

ISBN 3-211-36064-6
ISBN 978-3-211-36064-4

PREFACE

This volume contains the papers presented at the 16th Symposium on Theory and Practice of Robots and Manipulators, Warsaw, June 21–24, 2006. All papers had been reviewed by two independent reviewers before they were accepted for final publication and presentation at the Symposium. The event was organized under the supervision of international Steering Committee consisting of: M.Ceccarelli (IFToMM Secretary General, University of Cassino, Italy), I-Ming Chen (Nanyang Technological University, Singapore), B.Heimann (Chair of Technical Committee Robotics, Hannover University, Germany), E.Martin (Space Agency, Canada), O.Khatib (Stanford University, USA), W.Schiehlen (CISM representative, Technical University Munich, Germany), O.Takanishi (Waseda University, Japan), T.Zielińska (Warsaw University of Technology, Poland). Local Organizing Committee consisted of T.Zielińska, M.Olszewski, C.Zieliński, K.Kędzior from Warsaw University of Technology, K.Kozłowski from Poznań Technical University, and K.Tchoń from Wrocław Technical University. The symposium was held at the Faculty of Mechatronics, Warsaw University of Technology.

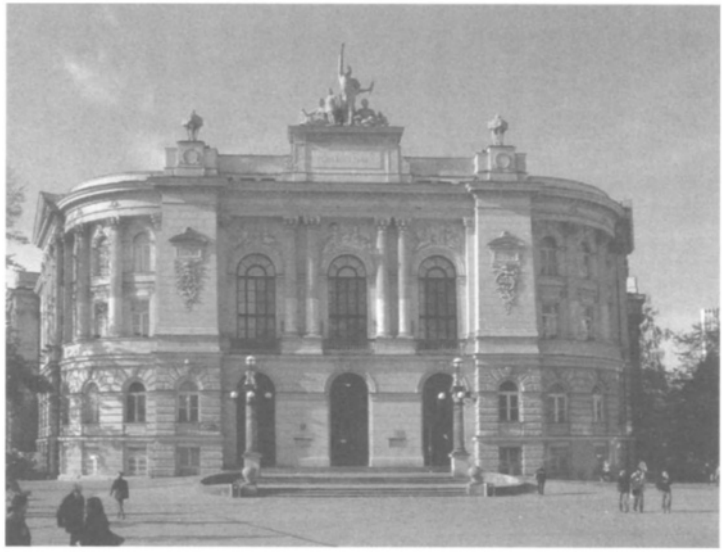

Main Building, Warsaw University of Technology

The 1st CISM-IFToMM Symposium on Theory and Practice of Robots and Manipulators was held on Sept. 5–8, 1973, in Udine, Italy, not long after IFToMM had been founded in 1969. The first ROMANSY, or Ro.Man.Sy, as the Symposium used to be referred to, marks the beginning of a long-lasting partnership between two international institutions, CISM, the Centre International des Sciences Mécaniques, and IFToMM, the International Federation for the Promotion of Mechanism and Machine Science. ROMANSY is one of the activities of IFToMM Technical

Committee for Robotics. The Symposium has taken place every even-numbered year with only one exception for the first symposium. It is traditionally a limited gathering of scientists that encourages informal discussions and focuses on recent trends and advances in robotics. The volume is organized into nine chapters with more than 50 papers in all. The Authors from 17 countries discussed the problems grouped in the following thematic parts:

— *Robot Design, Mechanism Performance,*
— *Motion Planning and Synthesis,*
— *Control Methods and Systems,*
— *Humanoids,*
— *Biology and Robotics – Specialized Tools and Methods,*
— *Innovative Technologies in Robotics,*
— *Space Robotics,*
— *Vision and Navigation.*

The key-note presentations dealt with the problems of the coexistence of humans and personal robots providing assistance to people in their housework, or to the elderly and the handicapped, as well as the robots working with or without human help in space missions. It is interesting that the cultural aspects influencing the robotics research also attracted the attention of the Scientists. Modeling and control methods of complex human-like robotic systems are developing very fast with the goal to produce a robot with human motion skills. To effectively work and cooperate with us, robots must exhibit abilities that are comparable to those of humans. The speakers focused on the ongoing efforts to design and develop human-friendly robotic systems that can safely and effectively interact and work with humans. The progress in robotics is also stimulated by human will to explore outer space. This issue creates specific requirements, limitations and targets for the designers. Standardization in space robots is necessary to enable the creation of advanced cooperative systems, where different technologies, requirements, control systems etc. meet. Finally, standardization is a critical element in having large numbers of robots working safely side-by-side their human counterparts.

*The 16th ROMANSY solicited papers providing a vision of the evolution of the robotics disciplines and identifying new directions in which these disciplines are foreseen to develop. The papers are devoted to novel robots, humanoids and bio-robotics problems, challenges in control and motion synthesis, kinematical and dynamical analysis of robotic systems, perception problems, space robots, and to other promising innovative mechanisms and technologies. We hope that the material included in this volume does not limit itself to just reporting the ongoing research, but will also stimulate the Reader to create new ideas and solutions, as: „**Every scientists is an artist and every artist is a scientist in a part**" (from: Summa Technologiae, by Stanisław Lem, 1964, Wydawnictwo Lubelskie).*

Warsaw, 20th May 2006

Teresa Zielińska
Cezary Zieliński

CONTENTS

Keynote Lectures

Humanoid Robotics, Culture and Society of Japan

Atsuo Takanishi

Department of Mechanical Engineering / Humanoid Robotics Institute, Waseda University

3-4-1 Ookubo, Shinjuku-ku, Tokyo 169-8555

Japan

Even though the market size is still small at this moment, applied fields of robots are gradually spreading from the manufacturing industry to the others in recent years. One can now easily expect that applications of robots will expand into the first and the third industrial fields as one of the important components to support our society in the 21st century. There also raises strong anticipations in Japan that robots for the personal use will coexist with humans and provide supports such as the assistance for the housework, care of the aged and the physically handicapped, since Japan is one the fastest aging societies in the world. Consequently, humanoid robots and/or animaloid robots have been treated as subjects of robotics researches in Japan such as a research tool for human/animal science, an entertainment/mental-commit robot or an assistant/agent for humans in the human living environment. Over the last couple of years, some manufactures including famous global companies started to develop prototypes or even to sell mass production robots for the purposes mentioned above, such as TOYOTA, TMSUK, SONY, HONDA, Mitsubishi Heavy, ZMP, etc. Most of those robots have some life-likeness in their appearances and behaviors. Why are so many Japanese companies developing humanoid robots? I believe there is a special reason which strongly relates to the national character of Japan in terms of the history, the religion and the culture of Japan. On the other hand, Waseda University, where I belong to, has been one of the leading research sites on humanoid robot research since the late Prof. Ichiro Kato and his colleagues started the WABOT (WAseda roBOT) Projects and developed the historical humanoid robots that are WABOT-1 and WABOT-2 done in the early 70s and 80s respectively. One of the most important aspects of our research philosophy is as follows: By constructing

anthropomorphic/humanoid robots that function and behave like a human, we are attempting to develop a design method of a humanoid robot having human friendliness to coexist with humans naturally and symbiotically, as well as to scientifically build not only the physical model of a human but also the mental model of it from the engineering view point. Based upon the philosophy, I and my colleagues have been doing researches on humanoid robots, such as the Biped Walking Robots, Emotion Expression Robots, Mastication Robots, Flute Player Robots, Speech Production Robots, etc. In this plenary speech, I will introduce the national character of Japan in terms of the historical, religious and cultural backgrounds of Japan, as well as the research philosophy of humanoid robotics, the design concept of the humanoid robots and its applications with the robots mentioned above as examples.

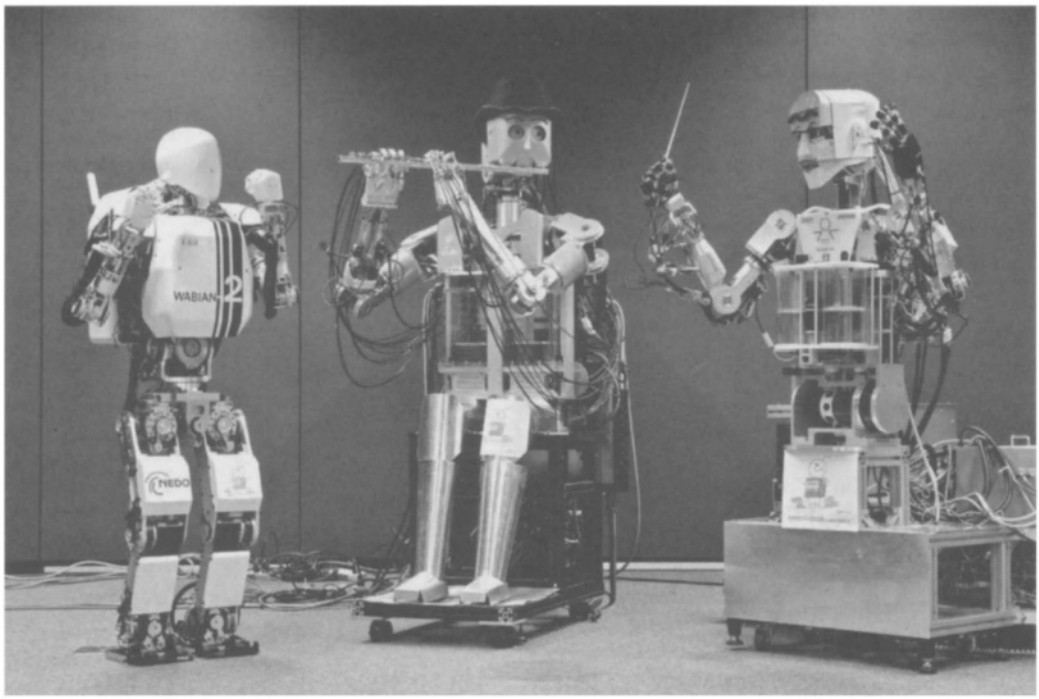

The Human Frontier: Robotics New Quest and Challenge

Oussama Khatib

Department of Computer Science
Stanford University, Stanford, California, USA
khatib@cs.stanford.edu

Summary

Robotics is rapidly expanding into human environments and vigorously engaged in its new emerging challenges. Interacting, exploring, and working with humans, the new generation of robots will increasingly touch people and their lives. The successful introduction of robots in these environments will rely on the development of competent and practical systems that are dependable, safe, and easy to use. To effectively work and cooperate with a person, robots must display abilities and skills that are compatible with those of humans. The discussion focuses on the ongoing effort for the design and development of human-friendly robotic systems that can safely and effectively interact and work with humans.

A major component in these developments is a new framework for the modeling and control of complex human-like robotic systems. In this framework, the various problems associated with (i) the motion coordination of the large number of degrees of such robots; (ii) the effective control of their contacts and interactions with the environment; (iii) the maintenance of their internal and external constraints; (iv) and the strategies for dealing with their underactuation and balance are all treated in a unified fashion within a general whole-body control structure. This is a task-oriented control structure that addresses the whole body dynamics for specifications involving multiple distributed tasks and postures in consistency with the requirements of multiple distributed contacts and constraints.

The second component in this effort is concerned with the synthesis of natural human movements to produce human-like robot behaviors. The objective is to unveil the underlying characteristics of human motion through an elaboration of its physiological basis. The aim is to formulate general strategies for whole-body robot behaviors. This exploration has employed models of human musculoskeletal dynamics and made use of extensive experimental studies of human subjects with motion capture techniques. Our

study of human motion has revealed the dominant role physiology plays in shaping human motion. The characteristics of human motion revealed in this study have allowed the development of generic motion creteria that efficiently and effectively encode human motion behaviors.

The third component in our effort is concerned with the critical issue of safety in robot design. Our work in human-friendly robot design has led to the development of a new actuation methodology which has been shown to be well-suited for the emerging generation of robots conceived to operate in human environments. This methodology of distributed macro mini actuation, DM^2, addresses both the safety and performance characteristics of a robot. The approach has led to the design and construction of several prototypes, the last of which is a two-arm on a common torso robotic testbed. This new system represents a unique platform to explore the competing issues of safety and performance in the design of robot mechanisms. The new two-arm torso testbed is being used to validate the promise of safety and performance and to establish meaningful measures for safety and performance. Of particular interest is the analysis of impact forces in a three dimensional collision between a robot and its surroundings. Two safety standard measures are used to quantify the improvement in safety in terms of reduction of impact force, while the robot performance characteristics are evaluated against traditional design.

Other fundamental issues in human-centered robotics will be also examined in this presentation. These include the elastic planning methodology for real-time modifications of existing plans, and various other effective methodologies and efficient algorithms that address the computational challenges associated with human-like robotic structures.

Standardization: A Logical Step in Sustained Space Exploration

Arthur Bradley[1]

[1] NASA Langley Research Center, USA, Arthur.T.Bradley@nasa.gov

Abstract. As NASA pushes ahead with its initiative to create a sustainable campaign of space exploration, there is a growing recognition that a paradigm shift will have to occur in the space robotics industry. Specifically, robotic systems-of-systems must be realized through a renewed focus towards interoperability, modularity, and commonality. The practice of developing unique mission-specific robots operating independently and communicating through custom interfaces will have to give way to standardization.

1 Motivation

In January of 2004, NASA was given a presidential directive to "gain a new foothold on the moon and to prepare for new journeys to the worlds beyond our own." As part of this initiative, NASA is focused on returning to the moon by 2020 to serve as the launching point for missions beyond. Robotic probes are expected to be on the lunar surface by 2008, with a human mission following as early as 2015, "with the goal of living and working there for increasingly extended periods of time." Based on this mandate, NASA published the Vision for Space Exploration (VSE), a roadmap for achieving sustainable exploration. In 2005, NASA's Exploration System Architecture Study (ESAS) subsequently recommended that robotics development focus on three things: (1) human-robot interaction, (2) material handling and transportation, and (3) improved surface mobility.

The focus of lunar and Martian expeditions will migrate from early exploration, to site preparation, to long-duration habitation. Given the hostile environmental conditions, each of these activities will require the extensive use of robotic systems. Such ambitious objectives will introduce tremendous new challenges – requiring system planners to think far beyond simply getting to the remote location safely and making scientific measurements or taking high-resolution photographs. Robots that operate independently of one another, like those seen in the past (e.g. Sojourner, Spirit/Opportunity), will be inadequate to accomplish the complex tasks associated with these challenges. Rather, complex systems-of-systems will be required in which robots work cooperatively by widely exchanging information, planning and dividing complex tasks, sharing common resources, and physically cooperating to manipulate objects. The challenges associated with cooperative robotics are many, including communications, smart mechanisms, control, autonomy, physical compatibility, sensor processing, and operator control.

In this paper, we describe the issues considered by an early investigation (i.e. JTARS) into standardization of space robotics. The benefits, scope, and steps necessary for enabling advanced cooperative systems are all briefly discussed.

2 Joint Technical Architecture for Robotic Systems

In 2005, NASA's Office of Exploration Systems Research & Technology funded the development of the Joint Technical Architecture for Robotic Systems (JTARS). JTARS charter was to identify the interface standards necessary to achieve interoperability among space robots. The working group was made up of recognized leaders in the field of space robotics including representatives from seven NASA centers along with academia and private industry. The working group's early accomplishments included addressing key issues required for interoperability, defining which systems are within the project's scope, and framing the JTARS standards manuals around classes of robotic systems. Unfortunately, a subsequent realignment within NASA left the JTARS effort without the broad participation necessary to complete the task. The working group is currently looking for follow-on opportunities to fund this valuable work.

3 Benefits of Standardization

There are many benefits to standardizing space robots. The most obvious benefits would come in the form of enhanced capabilities, cost savings, and risk reduction.

Enhanced Capabilities

Standardization would enable the creation of integrated robotic systems-of-systems that incorporate numerous individual units working cooperatively. Such complex systems would be capable of meeting the upcoming technical challenges, including off-planet resource handling (extraction, processing, and transport) and habitat development (construction, inspection, and maintenance). Standardization would also prove invaluable in developing systems that are capable of being controlled by universal (i.e. shared) operator control stations. Finally, standardization is a critical element in having large numbers of robots working safely side-by-side their human counterparts.

Cost Savings

Clear and relevant standards would serve as guidelines for acquisitions. Such standards would promote competition by effectively "leveling the playing field." This would allow for smaller companies to enter the market by reducing the high research costs associated with developing mission-unique systems. This increase in competition would ultimately lead to better product selection and cost reduction. It is also expected that standards-driven systems would be more modular in nature, leading to the sharing and reuse of components (both hardware and software). Finally, standards-based systems would be easier and cheaper to validate and verify through the use of common reusable test sets and simulators.

Risk Reduction

Significant risk reduction would result from replacing unique "one of a kind" systems with robots equipped with well-understood interfaces and capabilities. Reliability is also expected to improve as the designs mature and are subsequently reused. By increasing competition, the risks currently seen by being tied to a small set of vendors would also decrease. Finally, standards are expected to be "living documents," useful in distributing lessons learned, and thus helping to ensure that all vendors are aware of important design considerations.

4 Scope

The space community has many systems under development, from satellites to rovers, many of which can be considered "robotic" in nature. An important consideration of any standardization program is therefore to clearly define the scope of the effort, specifically answering the question, "What is a robot?" Two broad approaches have generally been considered. One divides systems based on where and how they are to be used, and the other divides systems based on capabilities.

The metrics considered descriptive of robotic systems by NASA's Joint Technical Architecture for Robotic Systems (JTARS) working group are: processing capability, communications, and the ability to physically interact with the world. Figure 1 illustrates how these three metrics are used to determine which systems fall within the scope of a standardization program.

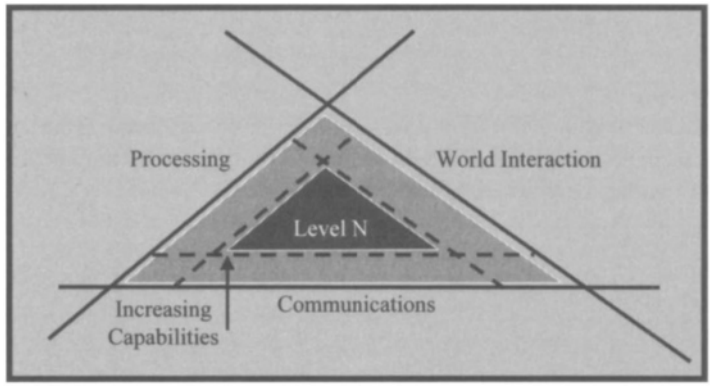

Figure 1. JTARS metrics used to define a "robot."

Systems that meet a minimum level of all three metrics would be considered robotic in nature and thus within scope. Within the core bounded region, sub-regions could also be identified to indicate systems with advanced capabilities. Additional requirements would likely be levied on more capable systems, enabling them to perform advanced cooperative activities. Therefore, it is expected that there would be different levels of compliance depending on system capabilities.

There are several important implications that result from this definition of scope. Specifically, the definition suggests that standards would be applied to robotic systems independent of their:

- Location (e.g. Mars, Earth, moon, in-space, etc.)
- Function (e.g. rovers, station crawlers, air vehicles, etc.)
- Level of autonomy (teleoperated to fully autonomous)

A broad inclusive definition of this nature removes the burden of asking the question "Does this robotic system need to be compliant?" Simply put, if the space system meets the minimum metrics defining a "robot," then it must be compliant to some minimum level, and perhaps a

greater level dependent on what cooperative tasks it will be assigned. An important exception however, is that standards requirements should not supersede higher-level heritage system-use requirements. For example, new maintenance robots to be used on the International Space Station (ISS) would have to be compliant with ISS requirements first and foremost, even at the expense of the goals of long-term standardization.

5 Enabling Cooperative Behavior

For robots to cooperate autonomously, as well as work with nearby astronauts, standardization must extend to the systems that interact with the robots. Examples of such systems include: end-effectors/tools, sensor suites, overhead satellites, operator control stations, communication networks, ground support equipment, and other cooperative robots. Complimentary systems of this nature must be capable of interfacing with robotic systems in a uniform way.

Four high-level topics have been identified as necessary for achieving robot standardization: physical interactions, information exchange, command structure, and reference frames.

Physical Interactions

Standards will need to identify physical interactions associated with robots working cooperatively, including (but not limited to) end effectors, tools, mounts and hard points, maximum loads, workspace constraints, and electrical mates.

Information Exchange

Defining the methods of exchanging information between robots and/or supporting systems requires the identification of interconnection standards, communication protocols, and message sets. The International Organization of Standards Open Systems Interconnection (OSI) 7-layer model is a good example of a top-to-bottom interconnection standard around which various protocols have been developed. The Department of Defense's Joint Architecture for Unmanned Systems (JAUS) is a relevant example of a message set designed for communications to/from robotic systems.

OSI Model

The OSI model defines a networking framework for implementing protocols in seven layers. Other variants (e.g. 5-layer) have also been proposed. With either model, control is passed from one layer to the next, starting at the application layer in one station, proceeding to the bottom physical layer, then over the channel to the next station and back up the hierarchy of the receiver. Additional information can be found at ww.iso.org.

JAUS Message Set

The Joint Architecture for Unmanned Systems (JAUS) was developed by the Department of Defense as a common message set between unmanned systems. It is currently being converted to a Society of Automotive Engineering (SAE) standard. JAUS addresses many of the important considerations of communicating between unmanned (robotic) systems, including:

- Commands/Sequences
- Responses
- Queries

- Data
- Events
- Periodic Communications

Command Structure

For robots to cooperative effectively, a command structure will also need to be defined. The command structure will serve as a policy for processing commands, sharing data, and changing the authority structure within individual units or across the larger system. The structure would define which system(s) have authority to direct subordinate systems. Figure 2 is a simple illustration showing how the command structure would influence the handling of incoming and outgoing information.

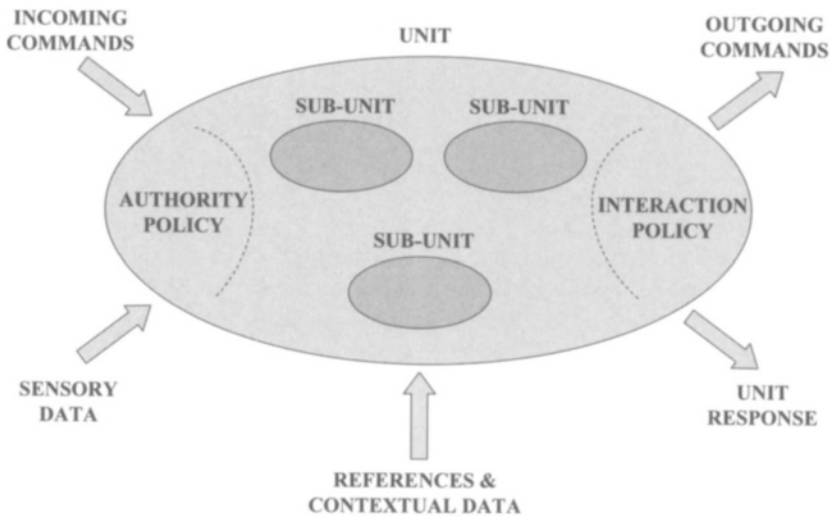

Figure 2. Command structure concept.

Reference Frames

Robotic systems working cooperatively will also require common frames of reference, including time, spatial distance, units of measure, and workspace definitions. Given the global collaboration in space activities, such definitions will have to address conventions that change across international boundaries.

Bibliography

United States Department of Defense Joint Technical Architecture, Vols. I and II, Version 6.0, October 2003.

Human and Robotic Technology Formulation Plan, Version 5.1, 29 July 2004 (Amended 13 September 2004), Development Programs Division, Office of Exploration Systems, National Aeronautics and Space Administration.

Technical Standards Program, information found at www.standards.nasa.gov.

Autonomy Levels for Unmanned Systems (ALFUS) Framework, *NIST Special Publication 1011*, September 2004.

Joint Architecture for Unmanned Systems, *JAUS Domain Model*, V3.0, December 2003.

Bradley, A., et. al., (2005). Enabling Interoperable Space Robots with the Joint Technical Architecture for Robotics Systems (JTARS), *8th International Symposium on Artificial Intelligence, Robotics, and Automation in Space*. Munich, September 2005.

Bradley, A., Holloway, C., *Final Report for Joint Technical Architecture for Robotic Systems*, submitted to NASA ESMD, January 2006.

Chapter I

Robot design

Design and Singularity Criteria of Parallel Manipulators

Victor Glazunov* and Alexander Kraynev*

* Mechanical Engineering Research Institute of RAS, Moscow, Russia,
e-mail: vaglznv@mail.ru

Abstract. This paper addresses the criteria of synthesis and singularity analysis of parallel manipulators. The dynamical decoupling, spatial oscillations as well as kinematic, static and dynamic singularities are considered. The proposed design criteria are intended only for dynamically decoupled manipulators whereas the singularity criteria can be applicable for general parallel manipulators.

1 Introduction

Parallel manipulators offer high stiffness and good position accuracy, they have been studied by numerous researchers. As it is said by J. Angeles (2004) "...the number of novel designs either published in conference proceedings and archival journals or disclosed in patent files is too rich to be recorded exhaustively". Let us mention only some books in which parallel manipulators are considered: Merlet (2000), Ceccarelli (2004), Glazunov, Koliskor, and Kraynev (1991). Most researchers have investigated maximal working volume or dexterous workspace (Chablat, Wenger, and Merlet, 2004, Glazunov and Munitsyna, 1994). In contrast with mentioned approaches other criteria (for example dynamical decoupling Kraynev and Glazunov, 1991, or reduction of the number of actuators in spatial oscillators Borozna, Glazunov, et al., 1992) involve different structures of parallel manipulators. To describe the various types of singularity Gosselin and Angeles (1990) have given the singularity criteria based on Jacobian matrices. Glazunov et al. (1990) proposed other singularity criterion based on the approach developed by Dimentberg (1965). This paper is focused on influences of the criteria mentioned above to corresponding results.

2 Dynamical decoupling

In this section, we represent the criterion of design of parallel manipulators taking into account the main motivation, which is the reduction of the dynamical coupling of the actuators. The basic idea is to represent the kinetic energy as the quadratic polynomial including only the squares of the generalized velocities.

Let us consider the Gough-Stewart platform. This manipulator is composed of a mobile platform connected to a fixed base via six kinematic sub-chains (legs) comprising one prismatic and two spherical pairs. Let the length of the i-th leg (the generalized coordinate) be denoted as l_i $(i=1...6)$.

The kinetic energy can be expressed by means of the 6×6 matrix (E) constituted by Plücker coordinates of the unit screws of the axes of the prismatic pairs:

$$(E)=\begin{pmatrix} x_1 & y_1 & z_1 & x_1^o & y_1^o & z_1^o \\ x_2 & y_2 & z_2 & x_2^o & y_2^o & z_2^o \\ . & . & . & . & . & . \\ . & . & . & . & . & . \\ . & . & . & . & . & . \\ x_6 & y_6 & z_6 & x_6^o & y_6^o & z_6^o \end{pmatrix} \tag{1}$$

Now let $(\dot{L})$ be the vector of the generalized velocities $(\dot{l}_1,\dot{l}_2,\dot{l}_3...,\dot{l}_6)^T$ and $\boldsymbol{\Omega}$ be the twist of the platform. The generalized velocities can be written as follows:

$$(E)\boldsymbol{\Omega}=(\dot{L}) \tag{2}$$

where $\boldsymbol{\Omega}$ is expressed as the vector $(v_x,v_y,v_z,\omega_x,\omega_y,\omega_z)^T$. Using the inverse matrix $(E)^{-1}$

$$(E)^{-1}=\begin{pmatrix} p_1^o & p_2^o & . & . & . & p_6^o \\ q_1^o & q_2^o & . & . & . & q_6^o \\ r_1^o & r_2^o & . & . & . & r_6^o \\ p_1 & p_2 & . & . & . & p_6 \\ q_1 & q_2 & . & . & . & q_6 \\ r_1 & r_2 & . & . & . & r_6 \end{pmatrix} \tag{3}$$

the twist $\boldsymbol{\Omega}$ can be obtained as:

$$(E)^{-1}(\dot{L})=\boldsymbol{\Omega} \tag{4}$$

Let m be the mass and J_x, J_y, J_z be the inertia moments of the platform. Then assuming that the mass of the platform is much more than the masses of the legs and using the Eqs. (3),(4), the kinetic energy T cab be expressed as (see Dimentberg, 1965, Kraynev and Glazunov, 1991):

$$T=\frac{m}{2}\left[\left(\sum_{i=1}^{6}p_i^o\dot{l}_i\right)^2+\left(\sum_{i=1}^{6}q_i^o\dot{l}_i\right)^2+\left(\sum_{i=1}^{6}r_i^o\dot{l}_i\right)^2\right]+\frac{J_x}{2}\left(\sum_{i=1}^{6}p_i\dot{l}_i\right)^2+\frac{J_y}{2}\left(\sum_{i=1}^{6}q_i\dot{l}_i\right)^2+\frac{J_z}{2}\left(\sum_{i=1}^{6}r_i\dot{l}_i\right)^2 \tag{5}$$

where $\dot{l}_i$ *(i=1...6)* are the generalized velocities.
The Lagrange equations can be written as:

$$\frac{d}{dt}\left(\frac{\partial T}{\partial \dot{l}_i}\right)-\frac{\partial T}{\partial l_i}=Q_i \tag{6}$$

where Q_i are the generalized forces *(i=1...6)*.
The dynamical coupling can be determined using the Eqs. (6). The expression of each generalized force comprises all generalized velocities and accelerations.
In order to reduce the dynamical coupling we represent the kinetic energy as follows:

$$\begin{aligned} T=&\frac{m}{2}\left[\sum_{i=1}^{6}\left(p_i^o\dot{l}_i\right)^2+2\sum_{i=1,j=1,i\neq j}^{6}p_i^op_j^o\dot{l}_i\dot{l}_j+...+\sum_{i=1}^{6}\left(r_i^o\dot{l}_i\right)^2+2\sum_{i=1,j=1,i\neq j}^{6}r_i^or_j^o\dot{l}_i\dot{l}_j\right]+ \\ &+\frac{J_x}{2}\left[\sum_{i=1}^{6}\left(p_i\dot{l}_i\right)^2+2\sum_{i=1,j=1,i\neq j}^{6}p_ip_j\dot{l}_i\dot{l}_j\right]+...+\frac{J_z}{2}\left[\sum_{i=1}^{6}\left(r_i\dot{l}_i\right)^2+2\sum_{i=1,j=1,i\neq j}^{6}r_ir_j\dot{l}_i\dot{l}_j\right] \end{aligned} \tag{7}$$

According to the Eq. (7) the design criterion is defined so that the columns of the following matrix *(D)* are to be orthogonal:

$$(D)=\begin{pmatrix} p_1^o\sqrt{m} & p_2^o\sqrt{m} & \dots & p_6^o\sqrt{m} \\ q_1^o\sqrt{m} & q_2^o\sqrt{m} & \dots & q_6^o\sqrt{m} \\ r_1^o\sqrt{m} & r_2^o\sqrt{m} & \dots & r_6^o\sqrt{m} \\ p_1\sqrt{J_x} & p_2\sqrt{J_x} & \dots & p_6\sqrt{J_x} \\ q_1\sqrt{J_y} & q_2\sqrt{J_y} & \dots & q_6\sqrt{J_y} \\ r_1\sqrt{J_z} & r_2\sqrt{J_z} & \dots & r_6\sqrt{J_z} \end{pmatrix} = \begin{pmatrix} \sqrt{m} & 0 & 0 & 0 & 0 & 0 \\ 0 & \sqrt{m} & 0 & 0 & 0 & 0 \\ 0 & 0 & \sqrt{m} & 0 & 0 & 0 \\ 0 & 0 & 0 & \sqrt{J_x} & 0 & 0 \\ 0 & 0 & 0 & 0 & \sqrt{J_y} & 0 \\ 0 & 0 & 0 & 0 & 0 & \sqrt{J_z} \end{pmatrix} (E)^{-1} = (M)(E)^{-1} \tag{8}$$

From the theory of matrices it is known that to satisfy the design criterion defined above the rows of the inverse matrix $(D)^{-1} = (E)(M)^{-1}$ are to be orthogonal. From this, the following matrix *(E)* is proposed:

$$(E)=\begin{pmatrix} 0 & 0 & 1 & 0 & -\sqrt{J_y/m} & 0 \\ 0 & 0 & -1 & 0 & -\sqrt{J_y/m} & 0 \\ 1 & 0 & 0 & 0 & 0 & -\sqrt{J_z/m} \\ -1 & 0 & 0 & 0 & 0 & -\sqrt{J_z/m} \\ 0 & 1 & 0 & -\sqrt{J_x/m} & 0 & 0 \\ 0 & -1 & 0 & -\sqrt{J_x/m} & 0 & 0 \end{pmatrix} \tag{9}$$

The determinant of the matrix (9) can be written as:

$$\det(E) = 8\sqrt{J_x J_x J_x}\Big/ m^{3/2} \tag{10}$$

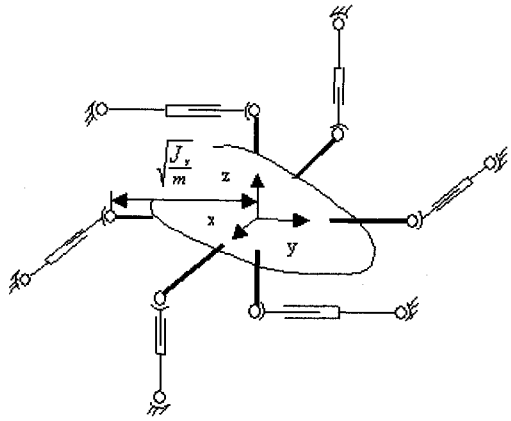

Figure 1. The parallel manipulator with dynamical decoupling.

In this case, the Eq. (5) can be simplified. The kinetic energy can be written as:

$$T = 0.25m\sum_{i=1}^{6}\dot{l}_i \tag{11}$$

Obtained matrix (9) corresponds to the Figure 1. Here the center of the mass of the platform coincides with the center of the co-ordinate system *xyz* and the axes of the legs are parallel to the

main central inertia axes of the platform. The proposed approach can be applicable for manipulators characterized by small displacements and high speeds.

3 Spatial oscillations

In this section, the parallel manipulator applicable as a spatial oscillator is considered. For instance such mechanism can be applied for testing electronic devices or as a flight simulator. It is clear that the well-known Gough-Stewart platform can be used for mentioned purposes. But this mechanism can cause several disadvantages because it is difficult to control six actuators in the compliance. From this, the criterion of design is introduced which defined as the minimum of the number of actuators. According to this criterion the device is proposed by Borozna, Glazunov, et al. (1992). In the Figure 2, the new mechanism is shown constructed by adding four universal joints situated between kinematic sub-chains.

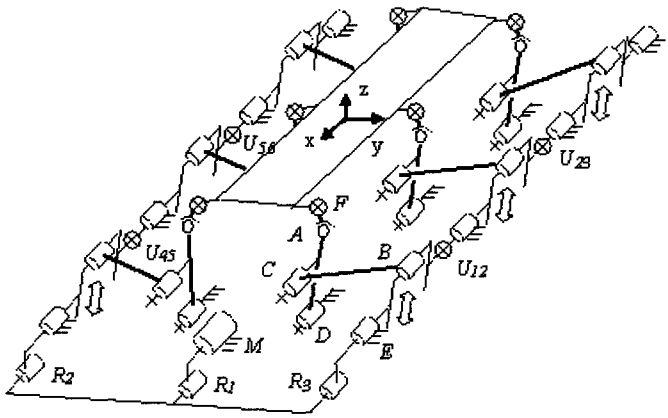

Figure 2. The parallel mechanism for spatial oscillations.

The mechanism consists of a platform connected to a fixed base via six kinematic sub-chains. The motor M situated on the base actuates the device by three rotating kinematic pairs R_1, R_2, R_3 and four universal joints U_{12}, U_{23}, U_{45}, U_{56}. Each kinematic sub-chain comprises a planar four-bar $B_iC_iD_iE_i$, the spherical pair A_i and the universal joint F_i $(i=1...6)$. The form of oscillations (the twist of oscillations) is determined by previous adjusting the lengths of the links B_iE_i. Since displacements of the platform are small, we use the linear equations to find the lengths of these links.

Let $\boldsymbol{\Phi}$ denote the required twist of the platform, $\boldsymbol{\rho_i}=(\rho_{xi}, \rho_{yi}, \rho_{zi})^T$ denote the vector directed from the origin to the point F_i, $(i=1...6)$. $\boldsymbol{\Phi}$ can be expressed by its Plücker coordinates $(\varphi_x, \varphi_y, \varphi_z, r_x, r_y, r_z)^T$. The displacement of the point F_i can be written as: $\boldsymbol{S_{Fi}}=(s_{Fx\,i}, s_{Fy\,i}, s_{Fz\,i})^T$ where

$$s_{Fx\,i}= r_x+ \varphi_y\rho_{z\,i} - \varphi_z\rho_{yi}, \quad s_{F\,yi}= r_y+ \varphi_z\rho_{xi} - \varphi_x\rho_{zi}, \quad s_{F\,zi}= r_z+ \varphi_x\rho_{yi} - \varphi_y\rho_{xi}, \tag{12}$$

Now let $\boldsymbol{L_i}=(L_{xi}, L_{yi}, L_{zi})^T$ denote the vector directed from the point A_i to the point F_i, $\boldsymbol{K_i}=(K_{xi}, K_{yi}, K_{zi})^T$ denote the unit vector along the displacement of the point A_i, and S_{Ai} denote the amplitude of this displacement. The latter can be written as:

$$S_{Ai} = l_{BEi}\, l_{ADi} / l_{CDi} \tag{13}$$

where $l_{BE\,i}$, $l_{AD\,i}$, $l_{CD\,i}$ are the lengths of the links BE_i, AD_i, CD_i, correspondingly *(i=1...6)*.
The projections of the velocities of the points A_i and F_i to the line A_iF_i passing through these points can be expressed as follows:

$$S_{A\,i}\, \boldsymbol{K_i L_i} = \boldsymbol{S_{Fi} L_i} \tag{14}$$

Using the Eqs. (12)-(14) the lengths $l_{BE\,i}$ of the links BE_i can be obtained *(i=1...6)*. If one of these lengths is more than the maximum $l_{BE\,max\,i}$ determined from design then all the lengths $l_{BE\,i}$ are to be multiplied by the coefficient $k = l_{BE\,max\,i} / l_{BE\,i}$.
Thus the parallel mechanism for spatial oscillations is presented that comprises only one motor. In proposed device the system of control is not needed to coordinate the displacements in the sub-chains.

4 Singularity criteria

Gosselin and Angeles (1990) have given the singularity criteria based on Jacobian matrices. Velocities of a parallel manipulator can be written in matrix form

$$(A)\dot{x} = (B)\dot{\theta} \tag{15}$$

where *(A)* and *(B)* are Jacobian matrices, $\dot{x}$ and $\dot{\theta}$ are absolute and generalized velocities correspondingly. According to the proposed criterion singularities exist if the determinants of the matrices *(A)* or *(B)* vanish.
It is known (see Mohammed and Duffy, 1985, Glazunov et al., 1990) that the matrix *(E)* (see the Eq. (1)) can be substituted into the Eq. (15). Each line in the matrix *(A)* can be interpreted as Plücker coordinates of the wrenches reciprocal to the unit vectors of passive joints of the corresponding kinematic sub-chains and the elements of the matrix *(B)* can be expressed as the mutual moments of the mentioned wrenches and the unit vectors of the actuated joints. Any element of the diagonal matrix *(B)* can be equal to zero if the unit vectors of all joints of this sub-chain are dependent. From this, the singularity criterion is proposed according to which singularities exist if the determinant *det(E)* of the matrix *(E)* comprising the Plücker coordinates of the reciprocal wrenches vanishes

$$det(E)=0 \tag{16}$$

or if the determinant consisting of the Plücker coordinates of the unit vectors of joints of any sub-chain vanishes. The condition (16) corresponds to the geometrical interpretation that six wrenches are reciprocal to the twist of possible infinite motion of the output link (see Dimentberg, 1965, Glazunov, Koliskor, and Kraynev, 1991). The criterion (16) brings opportunity to find the twists situated inside singularities.
Let us consider the Gough-Stewart platform, Figure 3. Let $\boldsymbol{\rho}_{Ai}=(x_{Ai}, y_{Ai}, z_{Ai})^T$, $\boldsymbol{\rho}_{Bi}=(x_{Bi}, y_{Bi}, z_{Bi})^T$ denote the vectors directed from the origin to the points A_i and B_i respectively *(i=1...6)*, l_i denote the distance between these points. Furthermore let $\boldsymbol{E}_i$ denote the unit screw situated along the *i*-th leg, $d\boldsymbol{\Phi}$ denote the twist of the platform. $\boldsymbol{E}_i$ consists of the unit vector $\boldsymbol{e}_i$ ant its moment $\boldsymbol{e}^o_i = \boldsymbol{\rho}_{Bi} \times \boldsymbol{e}_i$ and can be expressed by Plücker coordinates $\boldsymbol{E}_i = (x_i, y_i, z_i, x^o_i, y^o_i, z^o_i)$, as well as the twist $d\boldsymbol{\Phi} = (d\boldsymbol{\varphi}, d\boldsymbol{r}) = (d\varphi_x, d\varphi_y, d\varphi_z, dr_x, dr_y, dr_z)^T$.
An infinitesimal displacement of the point A_i can be written as: $d\boldsymbol{\rho}_{Ai}=(dx_{Ai}, dy_{Ai}, dz_{Ai})^T$ where

$$dx_{A\,i} = dr_x + d\varphi_y z_{A\,i} - d\varphi_z y_{Ai},\ dy_{A\,i} = dr_y + d\varphi_z x_{A\,i} - d\varphi_x z_{Ai},\ \ dz_{A\,i} = dr_z + d\varphi_x y_{A\,i} - d\varphi_y x_{Ai} \qquad (17)$$

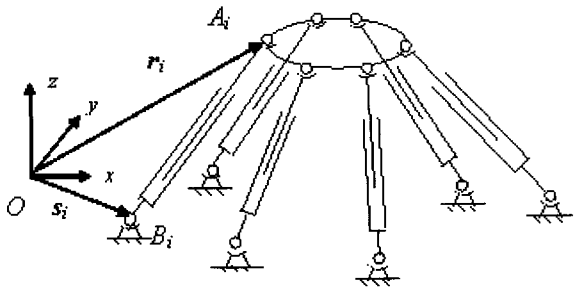

Figure 3. A parallel manipulator.

After this displacement the unit screw $\boldsymbol{E}_i$ can be rewritten (see Glazunov, Koliskor, and Kraynev, 1991, Glazunov et al., 2002) as $\boldsymbol{E}_i + d\boldsymbol{E}_i$ or as $\boldsymbol{e}_i + d\boldsymbol{e}_i$ and $\boldsymbol{e}^o_i + d\boldsymbol{e}^o_i$ where

$$d\boldsymbol{e}_i = [d\boldsymbol{\rho}_{Ai} - \boldsymbol{e}_i(d\boldsymbol{\rho}_{Ai}\boldsymbol{e}_i)]/l_i, \qquad d\boldsymbol{e}^o_i = \boldsymbol{\rho}_{Bi} \times d\boldsymbol{e}_i \qquad (18)$$

Using the Eqs. (17)-(18) the coordinates of the $d\boldsymbol{e}_i$ and $d\boldsymbol{e}^o_i$ can be expressed as:

$$\begin{aligned} dx_i &= (\partial x_i/\partial\varphi_x)\, d\varphi_x + (\partial x_i/\partial\varphi_y)\, d\varphi_y + (\partial x_i/\partial\varphi_z)\, d\varphi_z + (\partial x_i/\partial r_x)\, dr_x + (\partial x_i/\partial r_y)\, dr_y + (\partial x_i/\partial r_z)\, dr_z \\ &\cdots\cdots\cdots\cdots\cdots\cdots\cdots\cdots\cdots\cdots\cdots\cdots\cdots\cdots\cdots\cdots\cdots\cdots\cdots\cdots\cdots\cdots \\ dz^o_i &= (\partial z^o_i/\partial\varphi_x)\, d\varphi_x + (\partial z^o_i/\partial\varphi_y)\, d\varphi_y + (\partial z^o_i/\partial\varphi_z)\, d\varphi_z + (\partial z^o_i/\partial r_x)\, dr_x + (\partial z^o_i/\partial r_y)\, dr_y + (\partial z^o_i/\partial r_z)\, dr_z \end{aligned} \qquad (19)$$

where $\partial x_i/\partial\varphi_x = x_i(z_{Ai}y_i - y_{Ai}z_i)/l_i$, $\partial x_i/\partial\varphi_y = [z_{Ai}(1-x_i^2) + x_{Ai}x_iz_i]/l_i$, $\partial x_i/\partial\varphi_z = [y_{Ai}(x_i^2-1) + x_{Ai}x_iy_i]/l_i$,
$\partial x_i/\partial r_x = (1-x_i^2)/l_i$, $\partial x_i/\partial r_y = -x_i y_i/l_i$, $\partial x_i/\partial r_z = -x_i z_i/l_i$,
$\partial x^o_i/\partial\varphi_x = \{y_{Bi}[y_{Ai} + (z_{Ai}y_i - y_{Ai}z_i)z_i] + z_{Bi}[z_{Ai} + (y_{Ai}z_i - z_{Ai}y_i)y_i]\}/l_i$
$\partial x^o_i/\partial\varphi_y = \{y_{Bi}[(x_{Ai}z_i - z_{Ai}x_i)z_i - x_{Ai}] + z_{Bi}(z_{Ai}x_i - x_{Ai}z_i)y_i\}/l_i$
$\partial x^o_i/\partial\varphi_z = \{y_{Bi}(y_{Ai}x_i - x_{Ai}y_i)z_i - z_{Bi}[x_{Ai} - (x_{Ai}y_i - y_{Ai}x_i)y_i]\}/l_i$
$\partial x^o_i/\partial r_x = x_i(z_{Bi}y_i - y_{Bi}z_i)/l_i$, $\partial x^o_i/\partial r_y = [z_{Bi}(y_i^2-1) - y_{Bi}y_iz_i]/l_i$, $\partial x^o_i/\partial r_z = [y_{Bi}(1-z_i^2) - z_{Bi}y_iz_i]/l_i$, $i = 1\ldots6$.

Other partial derivatives can be obtained by index rotation.
By means of the properties of linear decomposition of determinants $d[det(E)]$ can be obtained as the sum of 36 determinants:

$$d[\det(E)] = \begin{vmatrix} \partial x_1/\partial\varphi_x & y_1 & z_1 & x_1^o & y_1^o & z_1^o \\ \partial x_2/\partial\varphi_x & y_2 & z_2 & x_2^o & y_2^o & z_2^o \\ \cdot & \cdot & \cdot & \cdot & \cdot & \cdot \\ \cdot & \cdot & \cdot & \cdot & \cdot & \cdot \\ \cdot & \cdot & \cdot & \cdot & \cdot & \cdot \\ \partial x_6/\partial\varphi_x & y_6 & z_6 & x_6^o & y_6^o & z_6^o \end{vmatrix} d\varphi_x + \ldots + \begin{vmatrix} x_1 & y_1 & z_1 & x_1^o & y_1^o & \partial z_1^o/\partial r_z \\ x_2 & y_2 & z_2 & x_2^o & y_2^o & \partial z_2^o/\partial r_z \\ \cdot & \cdot & \cdot & \cdot & \cdot & \cdot \\ \cdot & \cdot & \cdot & \cdot & \cdot & \cdot \\ \cdot & \cdot & \cdot & \cdot & \cdot & \cdot \\ x_6 & y_6 & z_6 & x_6^o & y_6^o & \partial z_6^o/\partial r_z \end{vmatrix} dr_x \qquad (20)$$

From this, $d[det(E)]$ can be represented as:

$$d[det(E)] = \partial[det(E)]/\partial\varphi_x d\varphi_x + \partial[det(E)]/\partial\varphi_y d\varphi_y + \ldots + \partial[det(E)]/\partial r_y dr_y + \partial[det(E)]/\partial r_z dr_z \qquad (21)$$

Using the Eq. (21) the criterion of determination of the singularity locus can be represented:

$$d[det(E)]=0 \tag{22}$$

This condition imposes only one constraint to motions of the platform therefore the singularity locus is 5-dimensioned for 6-DOF manipulators (and *(w-1)*-dimensioned for *w*-DOF manipulators). The determinant of the matrix *(E)* can be imagined as scalar function of six arguments that are the absolute coordinates of the platform. That is why all configurations corresponding to constant values of the determinant *det(E)* can be considered as hyper-surfaces of the constant level.

The Eq. (21) can be applicable for manipulators with actuation redundancy. It is apparent, that extra actuator must drive the manipulator from singularity as quickly as possible, i.e. along the twist-gradient $d\boldsymbol{\Phi}_g = (d\boldsymbol{\varphi}_g, d\boldsymbol{r}_g) = (d\varphi_{gx}, d\varphi_{gy}, d\varphi_{gz}, dr_{gx}, dr_{gy}, dr_{gz})^T$ where $d\varphi_{gx}=K\partial[det(E)]/\partial\varphi_x$, $d\varphi_{gy}=K\partial[det(E)]/\partial\varphi_y$, ... $dr_{gz}=K\partial[det(E)]/\partial r_z$, K is arbitrary coefficient. The condition (16) means that n *(n=2...6)* of 6 unit screws $\boldsymbol{E}_i$ enter in *(n-1)*-member group. This can be found by exception the row corresponding to the i-th joint $\boldsymbol{E}_i$. If remaining matrix is of the rank 5 then $\boldsymbol{E}_i$ is the member of mentioned group. The extra actuators must be placed only in corresponding sub-chains.

The method to avoid singularity can be based on the Eq. (22). Let ε denote the limit of *det(E)*

$$|det(E)|\geq\varepsilon \tag{23}$$

If a parallel manipulator is situated at a configuration where $|det(E)|=\varepsilon$ and the prescribed path corresponds to the desired twist $d\boldsymbol{\Phi}_d = (d\boldsymbol{\varphi}_d, d\boldsymbol{r}_d)$ leading to the next configuration where $|det(E)|<\varepsilon$ then the corrected twist $d\boldsymbol{\Phi}_c = (d\boldsymbol{\varphi}_c, d\boldsymbol{r}_c)$ can be determined. The components of this twist can be written as: $d\boldsymbol{\varphi}_c = d\boldsymbol{\varphi}_d - d\boldsymbol{\varphi}_g(d\boldsymbol{\varphi}_d\, d\boldsymbol{\varphi}_g)/(d\boldsymbol{\varphi}_g)^2$, $d\boldsymbol{r}_c = d\boldsymbol{r}_d - d\boldsymbol{r}_g(d\boldsymbol{r}_d\, d\boldsymbol{r}_g)/(d\boldsymbol{r}_g)^2$, where $d\boldsymbol{\varphi}_g$, $d\boldsymbol{r}_g$ are the components of the twist-gradient. The corrected twist $d\boldsymbol{\varphi}_c$ satisfies the condition (22) and is the nearest twist to the desired one. The Eqs. (16), (22), (23) express the kinematical criteria of singularity, moreover the Eqs. (16), (23) express the differential condition of singularity loci.

The static criterion of the configurations either singular or nearly singular is based on the pressure angles α_p which are angles between the forces acting along the axes $\boldsymbol{E}_i$ of the legs of parallel manipulators and the vectors of velocities or infinitesimal displacements of the corresponding points A_i (see V. Glazunov et. al., 1998). The six twists $d\boldsymbol{\Phi}_j$ *(j=1...6)* each of which is reciprocal with respect to five of the six unit screws $\boldsymbol{E}_i$ *(i=1...6)*, can be found to an accuracy of a scalar multiplier. If the twist $d\boldsymbol{\Phi}_i$ is known then the infinitesimal displacement $d\boldsymbol{\rho}_{Ai}$ of the point A_i can be obtained using the Eq. (17). The pressure angle α_{pi} is the angle between the vectors $d\boldsymbol{\rho}_{Ai}$ and $\boldsymbol{e}_i$: $\alpha_{pi}=|arccos(d\boldsymbol{\rho}_{Ai}\boldsymbol{e}_i/|d\boldsymbol{\rho}_{Ai}|)|$. Evidently that if $det(E)=0$ then $\alpha_{pi}=\pi/2$. Let φ_f denote the friction angle: $\varphi_f=arctg\, f$ where f is the coefficient of friction. The static singularity criterion is defined as:

$$\alpha_{p\,max}\leq\pi/2-\varphi_f \tag{24}$$

It is obvious that the working volume restricted by the kinematical criterion (16) is more than the volume restricted by the static criterion (24).

The dynamical criterion of singularity is determined taking into account not only geometrical but also inertial link parameters as well as control algorithm which must minimize the deviations of generalized coordinates from their program meanings (see Glazunov et al., 2004). This criterion is formulated as: the overrun of the generalized moment's marginal tolerance value. It is necessary that the moment surpass the nominal value not more than two times. On reaching such configuration there should be a load transfer with taking extra actuator into account. Note that certain configurations can be detected as singular or not singular by different criteria.

5 Conclusion

Thus, various criteria of design and singularity analysis of parallel manipulators are presented here. According to the criterion of the dynamical decoupling the kinetic energy is expressed as the polynomial including only the squares of the generalized velocities. The criterion of the design of the spatial oscillator is defined as minimum of the quantity of the actuators. The kinematic criterion of singularity corresponds to linear dependence of wrenches supporting the output link, the static criterion corresponds to the limitation of pressure angles and the dynamical criterion corresponds to the limitations of driving moments. Proposed criteria determine various results of synthesis and of detection of singularity of parallel manipulators.

Bibliography

J. Angeles. The Qualitative Synthesis of Parallel Manipulators. In *Journal of Mechanical Design,* 126: 617-624, 2004.

J.-P. Merlet. *Parallel Robots.* Kluwer Academic Publishers, 2000.

M. Ceccarelli. *Fundamentals of Mechanics of Robotic Manipulations.* Kluwer Academic Publishers, 2004.

V. Glazunov, A. Koliskor, and A. Kraynev. *Spatial Parallel Structure Mechanisms.* M.: Nauka, 1991.

D. Chablat, P. Wenger, and J.-P. Merlet. A Comparative Study between Two Three-DOF Parallel Kinematic Machines using Kinetostatic Criteria and Interval Analysis. In *Proceedings of XI World Congress in Mechanism and Machine Science,* Tianjin, China, pages 1209-1213, 2004.

V. Glazunov and N. Munitsyna. Optimal Design of Parallel Structure Manipulators for Extreme Environments of Textile Industry. In *Pr. of High Schools. Technology of Textile Industry.* 5: 85-89, 1994.

A. Kraynev and V. Glazunov. Parallel Structure Mechanisms in Robotics. In *MERO'91, Sympos. Nation. de Roboti Industr.,* Bucuresti, Romania, 1: 104-111, 1991.

Patent of Russia N 1753322 *The Six-Coordinate Vibration Stand* / A. Borozna, V. Glazunov et al. (G 01M 7/06), 1992.

C. Gosselin and J. Angeles. Singularity Analysis of Closed Loop Kinematic Chains. In *IEEE Trans. on Robotics and Automation,* 6(3): 281-290, 1990.

V. Glazunov, A. Koliskor, A. Krainev, and B. Model. Classification Principles and Analysis Methods for Parallel-Structure Spatial Mechanisms. In *Journal of Machinery Manufacture and Reliability,* Allerton Press Inc., 1: 30-37, 1990.

F. Dimentberg. *The Screw Calculus and its Applications in Mechanics.* M.: Nauka, 1965. (English translation: AD680993, Clearinghouse for Federal Technical and Scientific Information, Virginia).

M. Mohammed and J. Duffy. A Direct Determination of the Instantaneous Kinematics of Fully Parallel Robot Manipulators. In *ASME J. Mech., Trans., Autom. Des.,* 107(2): 226-229, 1985.

V. Glazunov, A. Kraynev, G. Rashoyan, R. Bykov, and N. Novikova. Neighboring Special Configurations of Parallel Manipulators. In *Theory and Practice of Robots and Manipulators. (RoManSy), Proceedings of XIV CISM-IFToMM Symposium,* Springer Wien New York, pages 59-66, 2002.

V. Glazunov, A. Kraynev, G. Rashoyan, and A. Trifonova. Design of the Paths of Parallel-Structure Mechanisms and Construction of their Working Zones with Allowance for Singular Positions. In *Journal of Machinery Manufacture and Reliability,* Allerton Press Inc., 5: 40-45, 1998.

V. Glazunov, A. Kraynev, R. Bykov, G. Rashoyan, and N. Novikova. Parallel Manipulator Control while Intersecting Singular Zones. In *Theory and Practice of Robots and Manipulators. (RoManSy), Proceedings of XV CISM-IFToMM Symposium,* Montreal, Canada, 2004.

L-legs for the Design of Mini and Micro Parallel Compliant Mechanisms

Matteo Zoppi and Rezia Molfino*
University of Genova, PMARlab, via all'Opera pia 15A, 16145 Genova, Italy.
{zoppi,molfino}@dimec.unige.it

Abstract. The paper presents a delocalized-compliance mechanism architecture, named L-gimbal, with 3 elastic equivalent degree of freedom and discusses three example applications of it characterized by the same degree of freedom requirements. The L-gimbal is a parallel mechanism realized using modular compliant leg elements named L-legs. It originates from a mechanism in IIM (Increased Instantaneous Mobility) singular configuration, showing that singularities can be exploited in synthesis of compliant mechanisms. The simple geometry of the L-gimbal makes it fit for fabrication with MEMS techniques. Three example applications of this compliant architecture are presented: an elastic joint for the steering-trust module of a worm robot with peristaltic locomotion, a micro wrist for minimally invasive robotic surgery, and an active MEMS mirror support.

1 Introduction

Mechanism and machine design is evolving in a multidisciplinary approach that simultaneously takes into account sensing, actuation and control issues for simultaneous satisfaction of functional and performance requirements. This evolution is mainly driven by the new paradigms of miniaturization of the products; easy, clean and low cost manufacturing; environment sustainability. A guiding concept is *functions fusion* resulting in integration of parts and subsystems each one contributing to make the overall structural, sensing and actuation functionalities merging/emerging in the complete system.

At design level, tools for multiphysics modeling, analysis and simulation are required for the concurrent definition of the parts of the system providing the different functionalities. Integration at physical level includes combination in the systems of multifunctional and new materials with specific characteristics. The fabrication process has a strong influence introducing additional design constraints. MEMS are an example.

Especially at smaller and MEMS scale, biomimetics is an effective approach. An important characteristics of bio mini and micro living creatures is the compliant structure of their invertebrate bodies.

Compliant mechanisms, composed of compliant and stiff elements realizing a desired mobility as the result of the elastic deformation of the whole structure rather than because

*Dr. Luca Bisio is kindly acknowledged for the help in the design of the worm robot module. The Italian Ministry of University and Research is acknowledged for the financial support.

of the relative displacement of the links (1), are an alternative to traditional mechanisms composed of kinematics pairs (i.e. revolute, prismatic, planar, etc.) and rigid (or almost rigid) links (*kinematics mechanisms*).

Some pros of compliant mechanisms compared to kinematics mechanisms are: minimum assembly needs; wider choice of shapes and geometric design parameters and materials for tailored applications; easy integration with modern (e.g. electrostatic, piezoelectric) actuators and smart materials; high reliability and MTBF (under fatigue life constraints); absence of joint friction, backlash and need of lubrication (but presence of a rest configuration and elastic forces); easier design for MEMS fabrication technologies.

We distinguish two types of compliant mechanisms: with localized and delocalized compliance.

Localized-compliance mechanisms are composed of rigid or almost rigid links and *localized-compliance joints*. They can be obtained from a kinematics mechanism (*reference mechanism*) in a certain configuration (*reference configuration*) by replacing the kinematics joints with compliant joints. Generally, in this case the compliant joints are designed to replicate at best the mobility of the kinematics joints they replace (same invariants and suitable distribution of stiffness), from which the name localized-compliance, e.g., for flexure hinges, minimum displacement of the rotation axis with the angle of rotation, stiffness about this axis low and rapidly increasing changing the axis of rotation (2; 3).

Any localized-compliance mechanism can be analyzed using the same methods and algorithms as for the reference mechanism, and the same kinematics models can be used, e.g. in the control system to compute the end-effector pose and displacement. Moreover, the actuators can be the same.

Localized-compliance mechanisms are the most used and studied today but applications exist where deformable structures with distributed (or *delocalized*) compliance (*delocalized-compliance mechanisms*) may result preferable. The paper deals with three such applications from the domain of robotics: • an elastic coupling in the steering-trust module of a worm robot with peristaltic locomotion; • a micro wrist for a new generation of small diameter surgical robots; • an active MEMS mirror support. All three applications are satisfied by the same compliant mechanism architecture, the L-gimbal, described in the following. As for kinematics mechanisms, the selection of a compliant mechanism architecture is mostly based on the desired mobility. In all three example applications considered, the required mobility is 2 rotational freedoms about a center of rotation O fixed to the base and 1 translational freedom (extrusion) in direction fixed to the end-effector.

In delocalized-compliance mechanisms, the mechanism structure as a whole provides the desired elastic constraint (4; 5). Compared to localized-compliance mechanisms, in general pros of delocalized-compliance mechanisms are larger mobility and higher reliability. On the other hand, delocalized compliance mechanisms may result less accurate and their synthesis and design much more complex (6). Because of these difficulties, even considering the recent advances in design methodologies, e.g. (7), an approach based on a-priori analyzed compliant modules and related heuristic design rules is advantageous.

In the selection of the delocalized-compliance mechanism presented in the paper, intelligent design rules including criteria like symmetry to achieve higher accuracy were

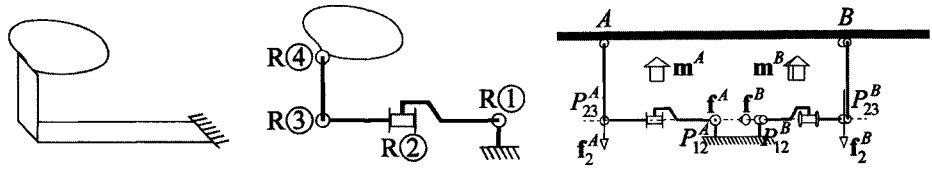

Figure 1. (a) L-leg: schematic (left) and the reference kinematics chain (right); (b) reference mechanism

adopted.

2 L-gimbal delocalized-compliance mechanism with L-legs

This section is devoted to the description of the L-gimbal mechanism and its modular legs; some hints are also given on the synthesis methodology, which starts from a parallel kinematics mechanism in singular configuration.

The L-gimbal is composed of two or more cylindrical elastic elements (compliant structures) with "L" shaped section, called *L-legs*, schematically represented in Fig. 1(a), connecting the end-effector to the base. The reference mechanism for the L-leg is the 4R serial chain in Fig. 1(a) in the shown reference configuration. A brief discussion of its mobility may be useful to understand the functioning of the L-gimbal (8).

The axes of the revolute joints are called $\boldsymbol{\xi}_i$, $i = 1, \ldots, 4$: $\boldsymbol{\xi}_1 \perp \boldsymbol{\xi}_2 \perp \boldsymbol{\xi}_3 \parallel \boldsymbol{\xi}_4$. The intersection point of $\boldsymbol{\xi}_1$ and $\boldsymbol{\xi}_2$ is called P_{12}; P_{23} is the intersection point of $\boldsymbol{\xi}_2$ and $\boldsymbol{\xi}_3$; π_{12} is the plane defined by $\boldsymbol{\xi}_1$ and $\boldsymbol{\xi}_2$. The system of structural constraint (with all leg joints free to move) applied by the leg in the reference configuration is a 2-system spanned by the pure force $\mathbf{f} \parallel \boldsymbol{\xi}_3$ through P_{12} and by the pure moment $\mathbf{m} \perp \pi_{12}$.

The reference mechanism for the L-gimbal is shown in Fig. 1(b) in reference configuration. The minimum number of legs to get the desired 3dof mobility is two (labeled with A and B in the figure), disposed with the axes of the base joints intersecting and not parallel, with the π_{12} coincident. The combined structural constraint applied on the end-effector (sum of the systems of structural constraints applied by the legs) is the 3-system spanned by $\mathbf{f}^A$, $\mathbf{f}^B$ and $\mathbf{m}^A$ (because $\mathbf{m}^A = \mathbf{m}^B$). Instantaneously, the end-effector tilts about axes in π_{12} through the center of rotation O at the intersection between $\boldsymbol{\xi}_1^A$ and $\boldsymbol{\xi}_1^B$, and translates in direction orthogonal to π_{12} (8). This configuration is a IIM (Increased Instantaneous Mobility) singularity (9; 10). Out of singularities the reference mechanism is 2dof; by selecting as reference configuration a IIM singularity it is possible to realize a 3 elastic dof deformable structure with the desired mobility. More details on the selection of the reference mechanism can be found in (8).

The third L-leg is added to realize a symmetric end-effector support: it increases the stiffness of the compliant mechanism without changing the stiffness distribution (low stiffness associated to the desired translations/rotations; high stiffness in the directions that have to be constrained). Moreover, in the symmetric system the displacements of the center of rotation associated with tilt mechanism partially compensate each-other.

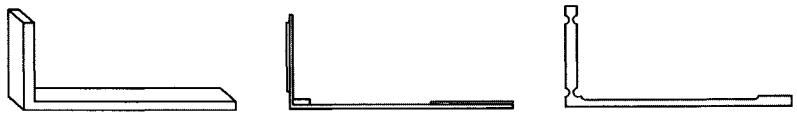

Figure 2. L-leg: alternative geometries

Different realizations of the L-leg are for example (Fig. 2): constant thickness elastic strip; layered, using materials with different stiffness characteristics; monolithic, variable thickness with grooves.

The same delocalized-compliance mechanism with purely parallel architecture, the *L-gimbal*, can be used in the three robotics applications presented in the following sections, which represent three realizations of the L-gimbal at meso, milli/micro and micro scale.

3 Worm robot steering-trust module

A modular worm robot with peristaltic locomotion for rescue applications is considered. The worm includes steering-trust modules, sensorial modules and a head module. The different modules are connected each other through modular interfaces allowing fast reconfiguration of the worm depending on the mission. Each module (except the head) is stand alone crossed by a power line and a bus. An umbilical connected to the back end of the robot provides power from a remote station and teleoperation commands. Electronics onboard the modules pilots the actuators and conveys sensor information in the bus.

The steering-trust compliant mechanism designed is shown in Fig. 3. In this module the 2 rotational freedoms are to bend the worm so making it steering, and the extrusion is needed to generate peristaltic trust.

The desired dimensions are: 45 mm diameter and 45 mm rest length, with 10 mm extrusion range and $\pi/18$ tilting angle.

The mechanism is composed of two L-gimbals connected in series (Fig. 3), which realize the desired elastic constraint between the two interfaces ⑤ and ⑥ of the module. The frame of each interface is a ring connected to three L-legs, whose other sides are fixed to the central yoke ④. Each L-leg is composed of two blades ① and ③ of superelastic alloy (for large bending) connected by an elbow vice ②.

Actuation is by SMA (shape memory alloy) wires ⑧ winded around two teflon rings ⑦, with lateral grooves to increase the wire lengths and thus the actuation range. Each wire pulls the corresponding elbow of the opposite leg. Because wires provide one-way actuation (they pull but do not push), the elbow vice angles are higher than $\pi/2$ allowing elastic preload of the module by assigning an initial tension to the actuation wires.

A measure of the effectiveness of the mechanism for this application is the ratio between shear stiffness (required low) and extrusion stiffness (required high). The final compromise value obtained is about 5.3. This is acceptable considering the high actuation forces generated by the SMA wires.

The center of rotation O is in the symmetry plane of the module, at the middle of the yoke ④. Some displacement of O associated with tilting is acceptable. The overall

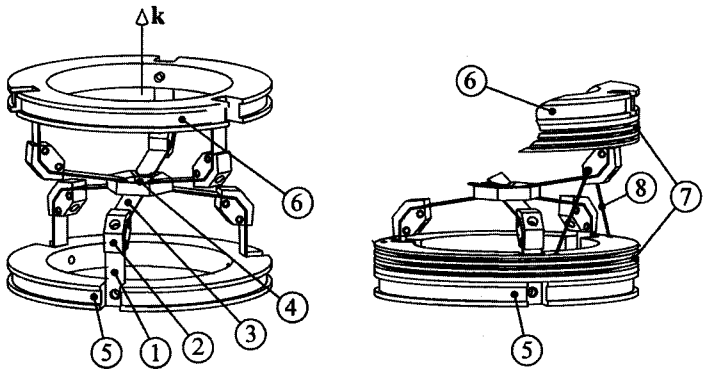

Figure 3. Worm robot steering-trust module: deformable structure of the module (left) and detail view of one actuation wire (right)

result is a robust and cheap mechanism fitting the application requirements. The use of a delocalized compliant mechanism instead of a kinematics or a localized compliant mechanism appears effective, in particular from the points of view of simplicity and large mobility ranges.

4 Micro wrist for minimally-invasive robotic surgery

The second example is at milli/micro scale.

Robotic systems for minimally invasive surgery provide outstanding benefits to the patients. Classes of surgical operations exist that could be carried out with surgical tools smaller than the ones today available in both traditional and robotic surgery. This pulls part of the research in the field of surgical robotics toward miniaturized surgical systems and one research subject is realization of micro wrists for manipulation of micro surgical instruments at the tip of a laparoscope (or other robotic system operating inside the patient).

Compliant mechanisms with parallel architecture, like the L-gimbal, can be particularly effective to get enough agility and stiffness in small dimensions and to keep the fabrication easy (11).

In the minimally-invasive surgical robotic wrist the 2 rotational freedoms are to orient the surgical instrument (e.g. a micro high-frequency electric knife), and the translational freedom is for fine movement of the instrument toward the tissues and backward, during the operation (the surgical robot carrying the wrist is supposed to provide rough positioning of the wrist in the operative region).

Wrist size and mobility considered are: 2 mm external diameter of the links of the surgical robot carrying the wrist (1.3 mm in diameter the wrist end-effector platform); 0.15 mm extrusion range and $\pi/9$ tilting angle.

Figure 4 shows the solution proposed. The L-legs (Fig. 4, right) are fabricated separately and assembled to the cylindric base ⑤ in grooves matching with the square leg

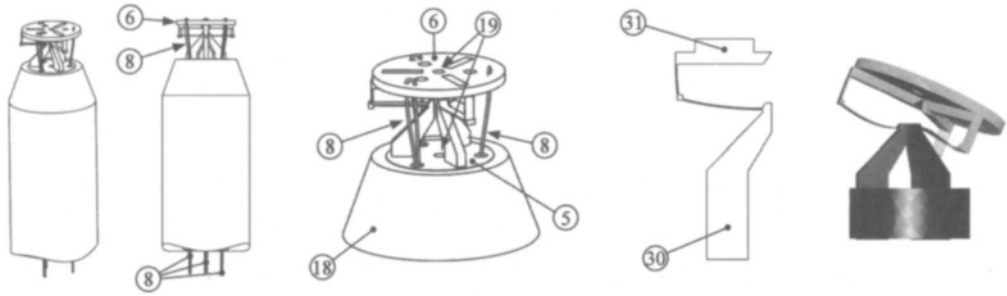

Figure 4. Wrist for surgical robot: full views; detailed view; profile of the L-leg; tilted configuration

ends ㉚. The end-effector platform ⑥ is assembled to the other leg sides ㉛. UV curing glue can be used for fixing the parts. The hole ⑲ in both base and end-effector, is to connect the surgical tool, fixed to the end-effector, to the base of the wrist, e.g. an electrical connection.

All parts are realized with LIGA technology (lithography, electroforming and molding for MEMS fabrication), depending on the aspect ratio.

The actuation proposed is by wires ⑧ pulled by actuators placed inside the link carrying the wrist or in the base of the surgical robot outside the patient. This solution presents several drawbacks such as difficulty to generate accurate movements and the fact that the wires provide one-way actuation, resulting in coupling of tilt and extrusion and in the need of an elastic preload of the legs for outward extrusion (opposite to the pulling direction of the cables). The main advantage of wires is the large actuation range achievable. Other actuations are considered, in particular SMA (Shape Memory Alloy) wires 25 μm diameter applying about 0.017 N pulling force. Figure 4, right, shows the wrist tilted by one wire at maximum force.

The surgical robot is teleoperated. During the operation, the small displacements of the center of rotation of the wrist can be compensated by the surgeon.

5 MEMS active mirror support

The third example, Fig. 5, is an application of the L-gimbal at a scale smaller than the surgical wrist.

The 2 rotational freedoms are required to tilt the mirror about the center of rotation O (reflection of a light beam) and the extrusion (orthogonal to the mirror surface) is for corrections at the wave-length scale of the reflected light such as compensating for nonplanarity in the wavefronts.

The first prototypes that we are realizing, in collaboration with the DXRL beamline Experiments Division of Elettra – Sincrotrone Trieste, to validate the concept have dimensions: 540 μm mirror diameter; 250 μm leg long side by 30 μm short side, 6 μm thickness, 40 μm largeness (aspect ratio about 7). Mirrors with these dimensions can be

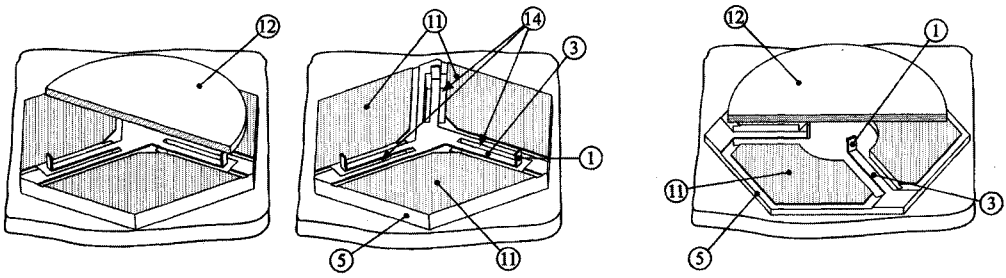

Figure 5. Micromirror active support: outward (a) and inward (b) architectures

easily fabricated using standard LIGA equipment. Then the system will be scaled down to 200 μm mirror diameter.

The main difference with the worm module and the surgical wrist presented in the previous sections is that, due to the size, the fabrication cannot include assembly operations.

The layer-by-layer fabrication starts from the mirror ⑫, Fig. 5(a) (the base layer is numbered ⑤, the legs ⑭). The horizontal ③ and vertical ① leg sides are realized in two steps: ③ in the same layer of the three electrode surfaces ⑪ used to command mirror tilt and extrusion by direct interaction (push/pull) with the mirror bottom surface.

Two leg placements are considered, providing same mobility: *outward* (Fig. 5(a)), with leg vertical sides at the periphery of the mirror and the leg-base connection at the center; *inward* (Figs. 5(b), left), with leg vertical sides at the center and leg-base connection at the periphery.

The fabrication process gives several design constraints, e.g. constant leg section, reducing the number of available design parameters (which can be used, for example, to reduce the displacement of the center of rotation).

The gap between electrodes and mirror can be reduced (in order to increase the electrostatic actuation forces) by fabricating the electrodes on an additional intermediate layer between the base and the mirror.

6 Conclusions

Two types of compliant mechanisms are introduced: localized-compliance mechanisms and delocalized-compliance mechanisms. Looking at applications where compliant mechanisms are preferable compared to kinematics mechanisms, the paper tries to underline that applications exist where delocalized-compliance mechanisms are preferable to localized-compliant mechanisms although their synthesis is more difficult. Reasons are larger workspace and easiness to fabricate, in particular at micro scale. Intelligent design, using modularity, symmetries to improve accuracy and new and smart materials can make things easier and lead to effective solutions. Control can play an important role, in particular for higher accuracy with control loops closed on the pose of the end-effector.

In this framework, a delocalized-compliance mechanism architecture, the L-gimbal, realized with three elastic leg elements called L-legs is presented and discussed. Three example applications are shown: Two already designed in detail and ready to be realized, the worm robot steering-trust module and the micromirror support; one, the surgical robotic wrist, at a development stage.

The surgical wrist and the worm module are presented in this paper for the first time.

In line with the proposed distinction between localized and delocalized compliant mechanisms, another type of smart mechanisms foreseen are deformable mechanisms with localized or delocalized (distributed) plasticity. Materials exist such as Cu–oxygen-free with virtually infinite fatigue life: they can be used to design structures almost without wear and fatigue failure.

Bibliography

[1] S. Smith. *Flexures, Elements of Elastic Mechanisms.* Taylor & Francis, London, England, 2000.

[2] J.M. Paros and L. Weisbord. How to design flexure hinges. *Int. J. Machine Design*, 37(27):151–156, 1965.

[3] N. Labontiu. *Compliant Mechanisms: Design of Flexure Hinges.* CRC Press, Boca Raton, FL, 2002.

[4] B. Trease, Y. Moon, and S. Kota. Design of large-displacement compliant joints. *ASME Int. J. of Mechanical Design*, 127(4):788–798, 2005.

[5] W. Weinstein. How to design flexure hinges. *Int. J. Machine Design*, 37(13-D):150–157, 1965.

[6] L.L. Howell. *Compliant Mechanisms.* Wiley, New York, 2001.

[7] G.K. Lau, H. Du, and M.K. Lim. Use of functional specifications as objective functions in topological optimization of compliant mechanism. *Int. J. Comp. Methods in Applied Mech. and Eng.*, 190(34):4421–4433, 2001.

[8] M. Zoppi and R. Molfino. Micro L-gimbal parallel mechanism for the active support of a micro mirror. In *36th Int. Symposium on Robotics ISR05*, Keidanren Kaikan, Tokyo, Japan, November 29 – December 1 2005.

[9] D. Zlatanov, R.G. Fenton, and B. Benhabib. A unifying framework for classification and interpretation of mechanism singularities. *ASME Journal of Mechanical Design*, 117:566–572, 1995.

[10] D. Zlatanov, I. Bonev, and C. Gosselin. Constraint singularities of parallel mechanisms. In *2002 IEEE International Conference on Robotics and Automation, ICRA 2002*, pages 496–502, Washington, DC, USA, May 11-15 2002.

[11] M. Zoppi, D. Zlatanov, and C.M. Gosselin. Analytical kinematics models and special geometries of a class of 4-dof parallel mechanisms. *IEEE Trans. on Robotics*, 21(6):1046–1055, 2005.

A singularity free parallel robotic mechanism for aiming antennas and cameras

Reg Dunlop[1], Michael Schlotter[2], Peter Hagedorn[2], Tim Jones[1],

[1] University of Canterbury, New Zealand reg.dunlop@canterbury.ac.nz
[2] Darmstadt University of Technology, Germany hagedorn@dyn.tu-darmstadt.de

Abstract. Several different mechanisms have been used to aim narrow beam communications links between earth stations and orbiting satellites. Only two axes are required to aim the beam but for the three conventional serially connected mechanisms currently used, a singularity about the first axis prevents tracking through a key hole region centered on the first axis and the communication link can fail. This key hole or mechanical singularity is caused by dynamic limitations which can never be overcome with the standard two axis serial mechanism. To keep the aim, it is common to add a third axis, or even add a two axis gimbaled base for marine applications. These serial connections reduce the stiffness of the aiming mechanism and increase the cost. A solution to this problem is to use a parallel robot. Previous work on two axis parallel robots showed that while such a mechanism could provide hemispherical coverage, a singularity in the drive linkages prevented full control of the coverage. A different drive system has been developed to avoid all singularities and is presented here for the first time. The results of dynamic simulations of the system in marine applications are presented to show reduced drive system loadings due to motion of the mounting base. This robotic mechanism is also capable of providing singularity free hemispherical aiming capability for aircraft mounted camera systems.

1 Introduction

Aiming systems provide the ability to point a camera, antenna or weapon in a particular direction. The parallel robotic aiming mechanism to be discussed is shown in Figure 1. It is development of the constant velocity joint given by Hunt (1978) who in turn attributes it to Clemens (Steeds 1940). More recently the mechanism has been used as a wrist and as a joint for a bipedal walking machine (Sellaouti and Ouezdou 2005). The discussion is restricted to the problem of aiming an antenna but applies equally well to other situations. The aiming device is required to point the antenna in a direction

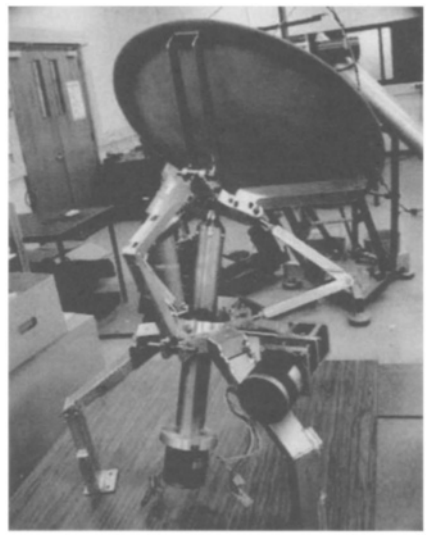

Figure 1. Parallel robot aiming system.

specified by the bearing and elevation or more generally the look angles as shown in Figure 2. Satellite tracking systems were developed after space research programs started in the late fifties. Monopulse tracking systems are widely used at many earth stations throughout the world (c.f. Hawkins et. al. 1988). Typically earth station antenna dish diameters vary from 10m to 30m and they can weigh several hundred tons. As the electromagnetic frequency used increases, the beam width is reduced and the accuracy required to track the satellite is increased.

In marine environments, this is even more difficult because the roll and pitch of the ship changes the direction of an antenna pointed at a communications satellite. The gain of the antenna is usually reduced to widen the beam width so that misalignment does not affect the signal as much. However, the transmission power of both the satellite and the earth station must be increased to compensate for the reduced antenna gain or else the data rates reduced to compensate for the reduced signal to noise. Such power increases are very costly, especially for the satellite end of the link. The degraded signal to noise ratio is not so important for voice communication, as speech contains considerable redundant information and context cues. For data communication, transmission rates are greatly reduced and retransmission is often necessary to correct errors.

In the next section, the standard serially connected mechanisms for mounting an antenna are described. This is followed by a section on parallel mechanisms outlining the capabilities and the limitations of such mountings. A two axis parallel mechanism is then described along with a drive development that provides singularity free hemispherical coverage. Finally simulation results for using such a device on a rolling and pitching ship are presented.

2 Standard Mounting Systems

The azimuth (Az) and altitude (Alt) or elevation angles of the satellite viewed from the earth's surface are shown in Figure 2. The azimuthal plane is rotated about a vertical axis through the earth station so that the satellite is in the plane. The azimuth angle is measured eastward from geographic north, and the elevation angle in the azimuthal plane is measured from the horizon to the satellite. The antenna mounting is used to aim the antenna along the look angles so that the satellite is within the beam of the antenna. There are three standard 2 DOF mounting methods for achieving this. These are the Alt-Az, the X-Y, and the astronomical mountings; all of which were used for the early space object tracking antennas at the NASA Goldstone site in the U.S.

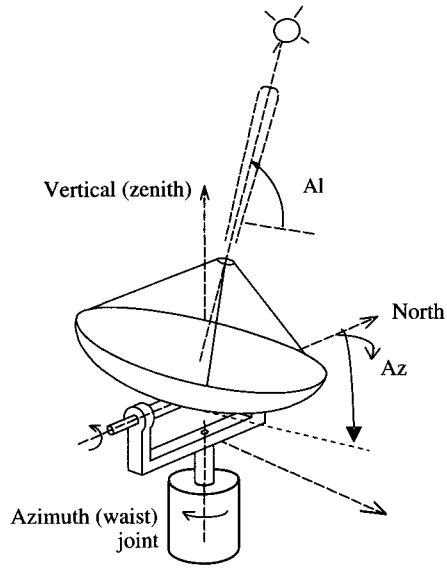

Figure 2. The Alt-Az antenna mount with the Alt-Az *look* angles as shown.

2.1 Alt-Az mountings - the key hole

The standard Alt-Az mount shown in Figure 2 consists of a horizontal axis revolute joint, which is attached to the rear of the antenna and carried on a vertical axis revolute joint. The look angles are set by rotating the vertical base joint through the azimuth angle from North, and then rotating the horizontal joint through the elevation angle from the horizon. If a moving satellite is tracked close to the zenith but not through it, then as the elevation nears 90^{o} degrees the azimuth has to rotate through 180^{o} degrees. During the time taken for the 180° degree azimuth rotation, the satellite moves out of the beam and the station loses contact. This is known as the key hole problem. While the problem can be anticipated and the azimuthal rotation started early, this only reduces the problem but does not eliminate it (Crawford and Brush 1995).

The problem occurs when the satellite track is through a region close to the zenith as there is a large change in one of the positioning coordinates for a small change in the satellite position i.e. adjacent look angles do not map into adjacent points in the control space. Thus, the system has a singularity about the zenith. The singularity or key hole problem is also known as gimbal lock in weapons systems and slew rate limiting in control system terminology.

For a tracking system mounted on a ship, the problem is particularly severe. The rolling and pitching action action causes the singularity of the alt-azimuth mount to trace out a conical region. Communication within this conical region is unreliable due to the effective increase in size of the key hole. Similar problems can arise with wind loading and vibrations on large narrow beam antennas.

2.2 X-Y and Astronomical mountings

In order to overcome the effect of having a key hole about the vertical axis, the first axis can be set at a different angle. For the X-Y mounting system the axis is horizontal as shown in. Figure 3. For the X-Y mount, each look angle affects both control angles, i.e. the axes are not decoupled and control is more complex. The advantage of the X-Y mount is that it does not have a key hole about the vertical, but it does have two other key holes: one at each end of the first (horizontal) axis. It is effectively the same as the Alt-Az system tipped on its side. When receiving signals from deep space probes, there is only one chance of capturing the data sent by the space craft and a loss of contact is not acceptable. In the case of the NASA deep space exploration antennas, two X-Y mounted antennas (10m and 30m at the Goldstone site) are mounted at each of the three receiving sites. At each site, the horizontal axes of the two antennas are orthogonal so that the key hole of each antenna is covered by the other antenna. This is an effective but expensive solution to the key hole problem.

For astronomical mounts, the first axis is parallel to the earth's N-S axis so when rotated at 1 revolution per day, the stars appear stationary. However, the singularity still remains but it is not a problem for star observations.

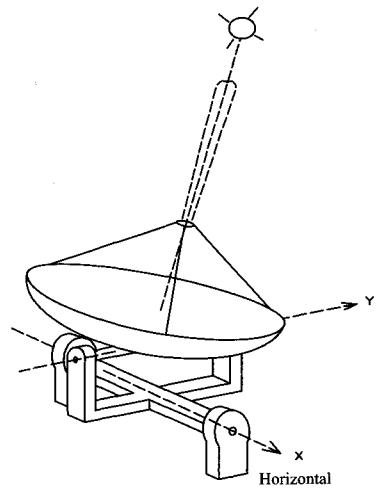

Figure 3. The X-Y mount.

2.3 Marine multi-axis mountings and key holes

The introduction of a third degree of freedom to overcome the limitations of a two axis mount in the vicinity of a key hole is used in marine communication mounting systems, and is quite common in earth resource and weather satellite tracking systems (cf. Johnson 1978). However, the increased mechanical complexity is costly and the axes must be computer controlled so that the mechanical singularities, which cause the key hole, can be avoided. The tracking system key holes are avoided by taking advantage of the extra degree of freedom to steer the mounting mechanism away from these singularities. Also the connecting revolute joints must be very stiff so as to avoid the cumulative errors associated with serial mechanisms.

More commonly, marine systems mount an Alt-Az antenna on a 2 axis gimbal giving a total of four degrees of freedom. The addition of extra serially connected joints to overcome the key hole problem (cf. CCIR report 1978) is expensive. The mass of the extra joint leads to an increase in the mass to be moved. Thus the supporting structure's strength and rigidity must be increased, and the drive motors and gear boxes upgraded further increasing the mass to be controlled. Also the cumulative errors from the joint positioning must be reduced by more precise measurement and control. This requires additional increases in the structural rigidity, which in turn leads to even more mass. The situation is one of diminishing returns for the extra expenditure.

3 Parallel aiming mechanisms

Dunlop, Ellis and Afzulpurkar (1993) devised an extended angular range Gough-Stewart platform mechanism to carry an antenna. Full hemispherical coverage was achieved with this 6 DOF system which used the 4 redundant DOF to maximize the aiming stiffness of the system. However, although the 6 axes were identical, the cost of the extra 4 DOF was considered too great and work continued on other parallel aiming systems. A 3 DOF spherical positioning parallel robot was produced by Dunlop and Jones (1997) based on the constant velocity joint described by Hunt (1978) and is shown in Figure 5. Further work by Dunlop and Jones (1998) resulted in the 2 axis parallel mechanism built to evaluate aiming throughout the hemisphere.

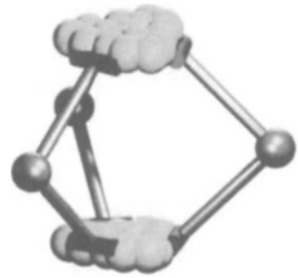

Figure 4. The basic 3 DOF parallel mechanism

4 Two axis parallel aiming mechanisms

The kinematics of the parallel 2 DOF aiming system shown in Figure 5(a) were developed to show the feasibility of the mechanism for a large angular range of movement (Dunlop and Jones 1998). However further investigation of the dynamics of this mechanism (Jones and Dunlop 2003) which included a counter weight (M) showed that a drive singularity occurred when the arms of the mechanism were driven to within 10° of the horizon. Some effect was expected as the symmetry of the mechanism was destroyed when only 2 of the 3 base revolute joints (R_1 and R_2) were driven. One approach was to use a pair of parallel connections to the central strut to

overcome the drive singularity problem but these prismatic joints could interfere with the antenna at some look angles. When moving the central strut, the moving platform that carries the antenna is set at the required position and the 3 parallel arms set the angular alignment for that particular position and thus aim the antenna. Using this approach resulted in the 2 DOF robotic mechanism shown in Figure 6(b).

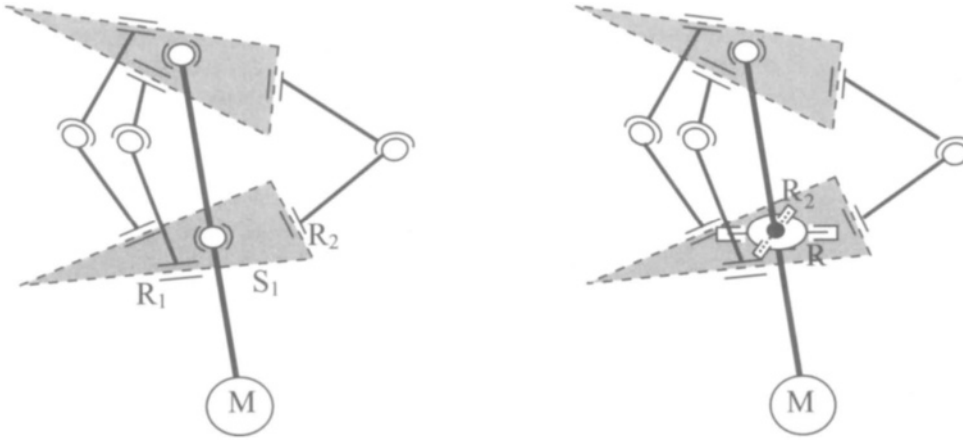

(a) (b)

Figure 5. Kinematics of the parallel 2 DOF aiming mechanism. The lower base triangle carries 3 revolute joints as does the upper platform triangle that carries the antenna. Spherical joints connect the arm pairs, and a central strut fixes the separation of the base and platform. Revolute joints R_1 and R_2 are driven. The spherical joint S_1 in the base of (a) has been replaced by a Cardan joint in (b) where both the Cardan revolute joints are driven as in an X-Y mounting.

Note that the mechanism in (a) has a mobility of 3 while (b) as only the required 2. The central strut in (a) is free to rotate and is a redundant unused DOF. The mechanism shown in Figure 1 is based on the kinematics in (b) and it demonstrated that the range of movement possible is more than that required for hemispherical coverage. The drives are applied via the Cardan joints to move the central strut which, for hemispherical coverage, is $< 45°$ from the vertical and hence well away from the 2 X axis singularities of an X-Y system drive. While the passive mechanism that orientates the antenna is parallel, the positioning system (that determines the operation of the angular alignment) is serially connected. The resulting mechanism is a hybrid mechanism with parallel orientation, and a serial position drive which is operated distant from its R_1 singularities.

5 Marine use of two axis hybrid aiming mechanism

The static counterbalancing requirements for the 2 DOF and 3 DOF systems with driven arms were analysed and while a large reduction in the torque required to move the parallel arms was achieved, complete balancing of the gravitational load was not possible at all positions (Dunlop and Jones 1996). When an aiming system is attached to a moving platform such as for a camera

mounted on a drone or an antenna on a ship, the translational movement of the base of the aiming mechanism affects the loading on the drives. A computational study was carried out to determine the dynamic drive requirements for a large antenna mounted on a rolling and pitching ship.

At the bottom of the central strut of the mechanism shown in Figure 1 (based on the kinematic diagram in Figure 5b) there is a single counterbalance weight comprised of the lead counterweights plus the second axis (R_2) drive motor. The counterbalance mass M can be varied and the effective position can be moved along the central strut. Static counterbalancing requires that the mass distance product be set, but dynamic balancing also requires the inertias be adjusted to be equal for the mechanism above and below the lower 2 axis gimbal (Cardan) joint. Because the antenna motion is different from the motion of the upper end of the central strut (i.e. the inertia dyadics differ significantly) perfect counterbalancing is not possible. Thus numerical simulation was used to determine the motor drive requirements for various counterbalance weights and positions.

For the mechanism shown in Figures 1 and 5(b), the object was to minimise the torque demands on the servo motors when the base was undergoing accelerations due to the vehicle movement. The simulation for the mechanism in Figure 1 used the Autolev software program (Kane and Levinson 1985, 2001) and the resulting C code was modified manually and compiled as a mex file for use in Matlab. The results were then output in graphical form. The parameters for all the mechanism components were included, and to indicate the scale, the distance from the driven Cardan joint to the drive motor/counter weight is 0.25m.

Results are presented in Figures 6 7 and 8 which show how the drive torques of the axes vary for the angular and linear accelerations used to simulate the motion of a ship. Figure 6 is a reference plot for no base acceleration. It is for tracking a target from -45° to + 45° about the first drive axis at 10°/s. A distinct minimum torque "valley" can be seen in Figure 6 and a suitable counterweight mass and position can be chosen along this valley. The remaining plots show the effect of base accelerations on the torque requirements for the drive motors.

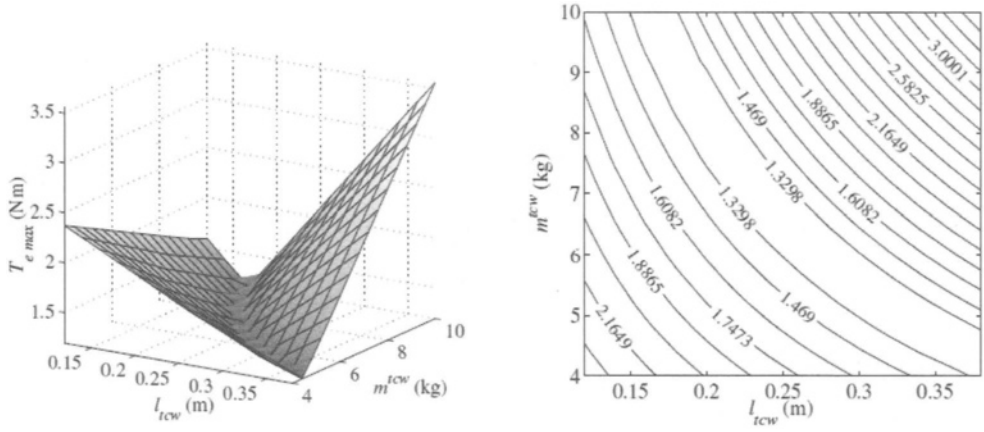

Figure 6. Magnitude of the first drive axis motor torque as a function of counterweight mass and position for tracking about the first axis at 10°/s from -45° to +45°.

The worst counterbalancing situation for the hybrid aiming mechanism occurs when the antenna is aimed horizontally. Figure 7 shows the effect of sinusoidal angular roll, pitch and yaw accelerations of the base over 10°, 8° and 2° with periods of 6.4s, 4.3s and 5.1s, respectively, and a vertical sinusoidal movement of amplitude 1.2m and period 4.3s. The tracker is aimed horizontally and the second axis is changing its position from 5° to 40°. Only the torque for the first motor is shown.

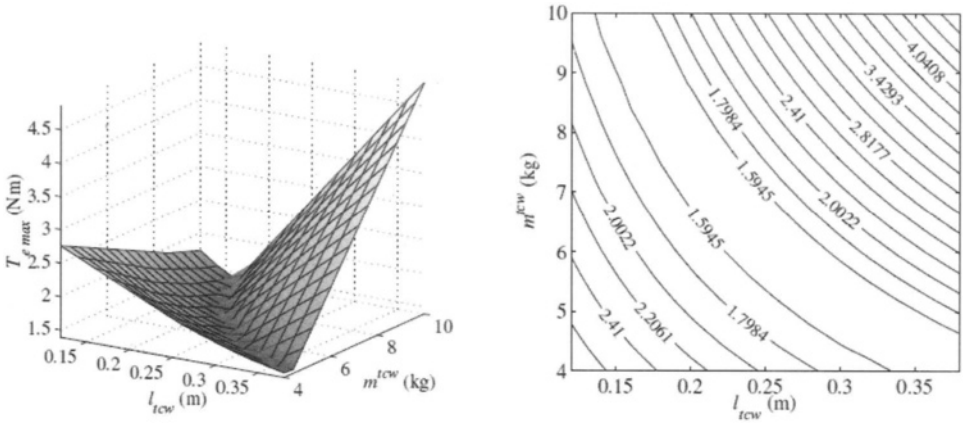

Figure 7. Magnitude of the first drive axis motor torque as a function of counterweight mass and position for tracking about the first axis at 10°/s from -45° to +45° while the base is undergoing angular and linear accelerations.

The effect of a conical scan in the presence of base accelerations is shown in Figure 8. It contains the results for the greatest torque required from either of the two drive motors while conducting a 360° azimuthal scan at an elevation angle of 30°. The base is undergoing the accelerations given for Figure 7, and the azimuthal scan rate is 15°/s.

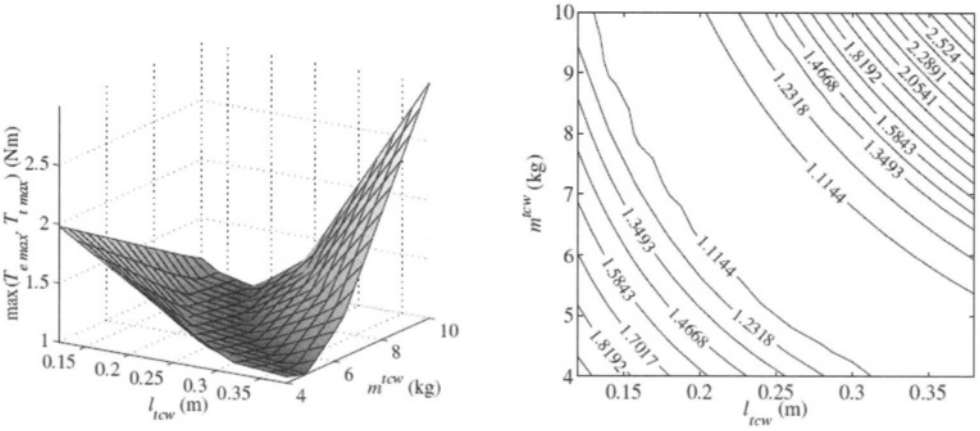

Figure 8. Magnitude of the largest motor torque of either drive axis as a function of counterweight mass and position for 360° azimuthal tracking with an elevation of 30° while the base is undergoing angular and linear accelerations.

Joint friction was also considered in the simulations and while it was found to have some effect on the basic positioning the extra effect when the base is accelerated is negligible as the mechanism is trying to keep the orientation of the antenna fixed i.e. it is not undergoing angular acceleration. Thus positioning is mostly to counter the base movements. In all 3 of the simulations presented, a desirable region for the counterweight mass and position is shown. Combining all 3 results for the aiming mechanism in Figure 1 showed that a counterweight of 6kg positioned 0.3m below the Cardan drive joints gives a satisfactory result.

6 Conclusions

A robotic mechanism combining the singularity free coverage of a 2 DOF parallel mechanism with the singularity free drive characteristics of a limited range X-Y aiming system has been presented. A small demonstration model of the system has been built and a range of simulations calculated for its performance in the presence of base accelerations similar to those experienced in marine applications. It was found that provided good static balancing is achieved, dynamic balancing is also satisfactory.

Bibliography

CCIR 1978 Mobile Services. Recommendations and reports of the CCIR XIVth plenary assembly, Kyoto, Volume VIII, Rep. 594-1, pp 381-399.

Crawford, P. S., and Brush, R. J. H. (1995). Trajectory optimisation to minimise pointing error, IEE Computing & Control Engineering Journal, Vol 6 (2) 61-67.

Dunlop, G. R., Ellis, P. J., and Afzulpurkar, N. V. (1993). The satellite tracking keyhole problem: a parallel mechanism mount solution, IPENZ Trans, Vol 20 (1) EMCh , 1-7.

Dunlop, G. R., and Jones, T. P. (1996). Gravity counterbalancing of a parallel robot for antenna aiming. *Proc. World Automation Congress,* ASME Press Series, ISBN 0-7918-0047-4, Vol 6, 153-158.

Dunlop, G. R., and Jones, T. P. (1997). Position analysis of a 3-DOF parallel manipulator. *Journal of Mechanism and Machine Theory*, Vol 32 (8) 903-920.

Dunlop, G. R., and Jones, T. P. (1998). Position analysis of a 2 DOF parallel manipulator. *Journal of Mechanism and Machine Theory,* Vol 34 (4) 599-614.

Hawkins, G.J., Edwards, D.J., and McGeehan, J.P. (1988). Tracking systems for satellite communications. Proc. IEE, Vol. 135/F (5) 393-407.

Hunt, K. H. (1978) Kinematic geometry of mechanisms. Oxford University Press, ISBN 0-19-856124-5, Fig. 13.8 p397.

Johnson, M. B. (1978) Antenna control system for a ship terminal for marisat. *Proc. Maritime and Aeronautical Satellite Communication and Navigation*, IEE Conference.

Jones, T. P., and Dunlop, G. R. (2003). Analysis of rigid body dynamics for closed-loop mechanisms - its application to a novel satellite tracking device. Proc. IMechE part1 JSCE, Vol 217 (14) 285-298.

Kane, T.R., and Levinson, D.A. (1985) *Dynamics: Theory and Applications,* McGraw-Hill.

Kane, T.R., and Levinson, D.A. (2001) Autolev user's manual. OnLine Dynamics Inc., www.autolev.com

Steeds, W. (1940). Mechanism and the kinematics of machines. Longmans, Green, London.

Sellaouti, R., and Ouezdou, F.B. (2005). Design and control of a 3DOFs parallel actuated mechanism for biped application. Mechanism and Machine Theory, Vol 40 (12) 1367-1393.